Journal of Controlled Release 385 (2025) 114053

Contents lists available at ScienceDirect

Journal of Controlled Release

journal homepage: www.elsevier.com/locate/jconrel

Lung tissue-optimized gene editing in human cystic fibrosis models following topical application of lipid nanoparticles

Belal Tafech [a,b], Tiffany Carlaw [a,b], Gaurav Sadhnani [c], Konrad Schmidt [c], Tessa Morin [a], Jerry Leung [d], January Weiner 3rd [c], Kevin An [e], Anita Balázs [f], Colin Ross [a], Dieter Beule [c], Marcus A. Mall [f,g,h], Hendrik Fuchs [i], Jay Kulkarni [e], Pieter R. Cullis [d,e], Sarah Hedtrich [a,b,c,j,*]

[a] Faculty of Pharmaceutical Sciences, University of British Columbia, 2405 Wesbrook Mall, Vancouver V6T 1Z3, BC, Canada
[b] School of Biomedical Engineering, University of British Columbia, Vancouver, BC, Canada
[c] Center for Biological Design, Berlin Institute of Health @ Charité, 13125 Berlin, Germany
[d] Department of Biochemistry and Molecular Biology, University of British Columbia, Vancouver, BC, Canada
[e] NanoVation Therapeutics, 2405 Wesbrook Mall, Vancouver, BC, Canada
[f] Department of Pediatric Respiratory Medicine, Immunology and Critical Care Medicine, Charité Universitätsmedizin Berlin, 13353 Berlin, Germany
[g] German Center for Lung Research (DZL), associated partner site Berlin, 13353 Berlin, Germany
[h] German Center for Child and Adolescent Health (DZKJ), partner site Berlin, 13353 Berlin, Germany
[i] Institute of Diagnostic Laboratory Medicine, Clinical Chemistry and Pathobiochemistry, Charité Universitätsmedizin Berlin, 13353 Berlin, Germany
[j] Centre for Blood Research & Life Science Institute, University of British Columbia, Life Sciences Centre, Vancouver, BC, Canada

ARTICLE INFO

Keywords:
Gene therapy
Gene editing
Lipid nanoparticles
Cystic fibrosis
Transmucosal delivery
Pulmonary gene delivery
CFTR

ABSTRACT

Cystic fibrosis (CF) is a severe monogenic disease characterized by debilitating lung dysfunction caused by loss-of-function mutations in the *CFTR* gene. While CRISPR-based gene editing holds promise for correcting these mutations and potentially curing CF, efficient delivery of gene editors to the lung epithelium through the mucosal barrier remains a major challenge.

In this study, we developed a lung-optimized gene editing strategy using lipid nanoparticles (LNPs) and evaluated it in increasingly complex, biomimetic human-based and patient-derived models. Systematic optimization of helper lipids, genetic cargo, guide RNA modifications, and gene editor ratios, alongside analysis of innate immune responses, achieved ~50 % editing efficiency in the model gene *HPRT* in two-dimensional models. Editing efficiency significantly dropped to ~5 % in biomimetic three-dimensional CF bronchial epithelial tissue models following topical LNP application. Pretreatment with the approved mucolytic agent dornase alpha increased editing efficiency to ~12.7 %. Finally, in CF patient-derived cells harboring the $CFTR^{R1162X}$ mutation, our optimized LNP formulation achieved ~12 % correction on gene level, offering a potential treatment avenue for this yet untreatable mutation.

Taken together, this study demonstrates that optimizing the genetic cargo as well as the delivery vehicle is key when striving for clinically applicable treatment approaches. It further provides insights into gene editing rates in human-based normal and CF patient-derived bronchial tissue models which express all relevant biological barriers and, thus, can pave the way for topically applicable treatment options for patients with CF and other genetic lung diseases.

1. Introduction

Cystic fibrosis (CF) is a highly debilitating and life-shortening monogenic disease that severely affects the lungs, pancreas, and other organs [1]. CF is caused by loss-of-function mutations in the cystic fibrosis transmembrane conductance regulator (*CFTR*) gene which results in the formation of highly viscous mucus hydrogels and impaired mucociliary clearance. This ultimately promotes severe lung infections [2], a decline of the lung function and respiratory failure, which remains the primary cause of death amongst CF patients [3,4].

The introduction of CFTR modulators, and especially the triple combination of elexacaftor-tezacaftor-ivacaftor, has markedly improved

* Corresponding author at: School of Biomedical Engineering, University of British Columbia, 2350 Health Sciences Mall, Vancouver, BC V6T1Z3, Canada.
E-mail address: sarah.hedtrich@ubc.ca (S. Hedtrich).

https://doi.org/10.1016/j.jconrel.2025.114053
Received 7 February 2025; Received in revised form 16 July 2025; Accepted 17 July 2025
Available online 18 July 2025

the treatment and prognosis of CF patients [4,5]. While CFTR modulators restore CFTR function in patients harboring F508del mutations, they remain ineffective in the ~10 % of CF patients that carry point CFTR mutations that are not amenable to CFTR modulation therapy [6]. Further, current CFTR modulators do not cure CF and partial restoration of CFTR function is associated with substantial persisting lung infection and inflammation [7–9]. Additionally, a life-long treatment is required which may be associated with distinct adverse effects [4].

Hence, further research is needed when aiming for an efficient treatment and cure for all CF patients. Exciting advances in CRISPR-mediated gene editing now provide us with powerful tools to treat and correct disease-causing mutations of previously untreatable conditions including CF. [10] As of today, it is theoretically possible to correct ~90 % of all known mutations using increasingly precise gene editing tools such as base or prime editors [11].

Yet, delivering the genetic cargo to its target site in the lungs remains a major challenge [12]. While systemic application of lung-targeting nanoparticles is explored [13], a topical application of the gene editors remains the most straightforward approach. However, the highly viscous and sticky lung mucus poses a very restrictive biological barrier. Normal airway mucus is composed of ~97 % water with the remaining 3 % consisting of mucins, salts, lipids, DNA, and cellular debris [14]. In CF patients, the mucus is significantly more viscous due to higher mucin concentrations (~10 %), resulting in smaller pore sizes, increased ionic concentrations, and lower pH values [1,15,16]. Notably, a doubling of mucin concentrations leads to a 6–10-fold increase in viscosity, which significantly hampers drug delivery [12,17–21].

Lipid nanoparticles (LNPs) are currently the most advanced non-viral gene delivery system yielding exciting preclinical and clinical data in delivering any type of RNA cargo [22,23]. Yet, we are lacking data that LNPs can effectively overcome the lung mucus in CF patients to edit the target cells in the underlying epithelium. While some studies demonstrate successful editing of the lung epithelium in rodents following topical and systemic administration, the translational value and predictivity of these findings for the human situation remains ambiguous due to distinct interspecies-related differences. In fact, the anatomical layout and cell composition of murine lungs is very different from humans and, importantly, rodents produce significantly less mucus [24–26]. Hence, the biological barriers present in these in vivo models often poorly represent human (patho)physiology.

In recent work from our lab, we identified critical LNP design criteria that facilitate the transmucosal delivery of gene editors to the lungs and result in clinically relevant gene editing rates in human epithelia [12,27]. Building onto this, here, we report an iterative approach yielding a lung-tailored gene editing strategy using LNPs. We exclusively worked with primary human cells and tissue models including CF patient-derived material to maximize the translational value of our study. We systematically investigated the impact of helper lipids, mRNA and single guide RNA (sgRNA) modifications, sgRNA:gene editor ratios as well as the impact of endosomal escape enhancers and immunosuppressants on the gene editing efficacy of the model gene *HPRT* in human (disease) models. This eventually enabled us to identify a setup that results in clinically relevant gene editing rates in human CF disease models, whereas pre-treatments with the clinically approved mucolytic dornase alpha doubled the editing efficacy. Finally, we demonstrate the potential of our lead LNP formulation to correct the point mutation $CFTR^{R1162X}$ in CF patient-derived cells for which no treatment options are currently available.

2. Results & discussion

2.1. Commonly used LNP compositions yield low editing efficacy in primary human bronchial epithelial cells

We first examined the transfection efficacy of LNPs composed of standard helper lipids (DSPC, DOPC and DOPE) and the clinically used ionizable lipid MC3 in primary human bronchial epithelial cells (NHBE). As expected, the transfection efficacy was ApoE dependent and increased with higher mRNA concentration (0.1–1 μg/mL) (Fig. S1). Further, DOPE-LNP resulted in the highest luciferase activity and functional GFP expression, respectively (Fig. 1A, B).

We next performed a head-to-head comparison of these LNPs loaded with Cas9 mRNA/sgRNA targeting the model gene *HPRT* with respect to gene editing efficacies. The latter was assessed via a qPCR assay, which determines the percentage of indel formation (small insertions or deletions of <50 base pairs) in the *HPRT* gene using intercalating dyes. In NHBEs, we detected 7–9 ± 3 % indels, whereas no significant differences between the LNP formulations were noted (Fig. 1C). Based on these data, we selected DOPE-LNP and 1 μg total RNA concentration as baseline for further experiments.

We next tested the editing efficacy of Cas9 ribonucleoprotein (RNP) compared to Cas9 mRNA. Since delivered in its active protein form that does not require translation from mRNA, higher editing rates have been previously reported [28,29]. RNP also caused less cytotoxicity compared to Cas9 mRNA (71–81 % whether encapsulated into RNAiMAX or DOPE-LNP) which is in line with previous data from our lab (Fig. 1D) [27].

We then assessed the editing efficacy of RNP-loaded DOPE-LNPs compared to mRNA-loaded DOPE-LNPs in NHBE cells. RNP-loaded formulations yield 6–10 ± 2 % indel formation (Fig. 1E), which did not differ significantly from mRNA-transfected cells. To benchmark the low editing rates obtained in primary human NHBE, we ran a comparison in the easy-to-transfect HEK293 cells. We achieved 46 ± 3 % indel formation in HEK293 cells, compared to 10 ± 2 % in NHBE, demonstrating that primary human NHBEs are indeed difficult-to-edit cells. It further demonstrates the poor predictive value of gene editing rates obtained in cell lines for primary human cells.

Interestingly, other primary human epithelial cells such as skin keratinocytes are significantly easier to edit indicated by editing rates >15 % using identical LNP formulations [27]. Other groups have reported similar findings [30,31], including the lack of editing following RNP transfection with commercial transfection reagents [32]. This prompted efforts to utilize alternative, peptide-based delivery systems [32], lentiviral transduction followed by the selection of edited cells, or electroporation [33–35], the latter of which however is not suitable for in vivo applications.

To determine if the gene editing efficacies increase when applying higher total RNA concentrations, we delivered up to 10 μg/mL total Cas9 mRNA/sgRNA to NHBEs via LNP. While this did not increase the indel formation overall, it even decreased at 10 μg/mL total RNA (Fig. 1F). Interestingly, the cell viability remained largely unchanged across the tested RNA concentrations (Fig. 1G) indicating that the reduced editing efficacy at high RNA concentrations are due to mechanism other than cytotoxicity.

2.2. Unmodified Cas9 mRNA triggers strong pro-inflammatory responses in primary human lung epithelial cells, yet these are not causal for the low editing rates

The lung epithelium is a first defense line of the human body and as such has developed unique mechanisms to protect it from foreign material and pathogens such as distinct RNA sensing and processing mechanism [36]. Striving to understand the underlying reasons of the low gene editing efficacies in NHBE, we assessed the immunogenicity of different Cas9 formats and subsequently its impact on gene editing efficacy.

It is well established that when tissues and cells sense foreign RNA, interferons are produced which hamper mRNA translation [37]. We therefore investigated the impact of unmodified and pseudouridine-modified Cas9 mRNA and Cas9 RNP on the innate immune response of NHBE. Bulk RNA-Seq analysis revealed substantially different gene expression profiles for unmodified and pseudouridine-modified mRNA

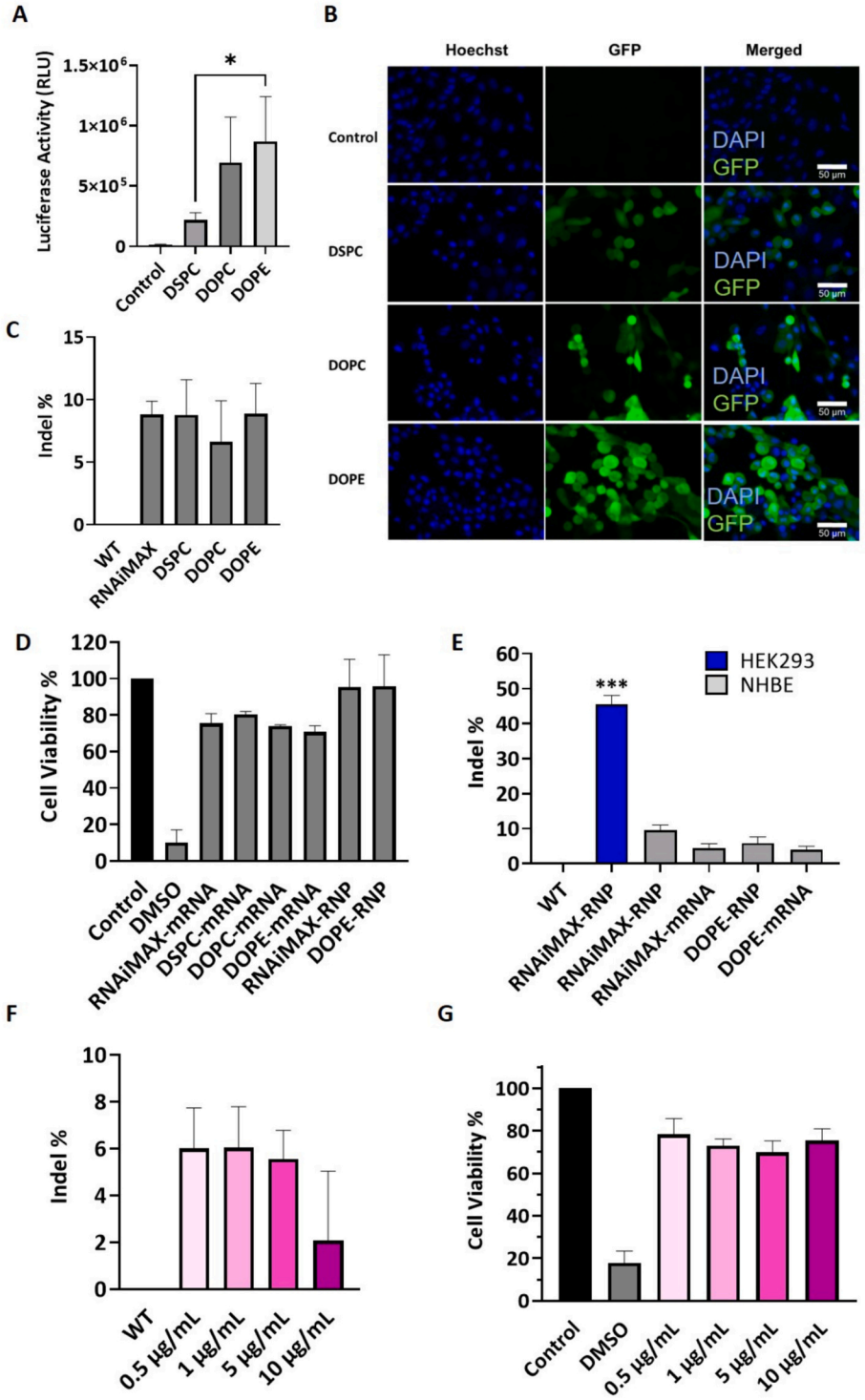

Fig. 1. A) LNPs containing the helper lipids DOPE, DSPC and DOPE loaded with luciferase mRNA and transfected into primary human bronchial epithelial cells (NHBEs). After 24 h, the luciferase activity was measured as relative light units (RLU). B) Representative fluorescence microscopy images comparing functional GFP expression 24 h after transfection of NHBEs with DOPE, DSPC, and DOPC-LNP. C) Frequency of indel formation in % (normalized to wild-type (WT) cells) in the model gene *HPRT* after transfection of NHBEs with Cas9 mRNA-loaded LNPs. D) Cell viability of NHBEs 48 h after treatment with RNAiMAX, DOPE-, DOPC-, and DSPC-LNP loaded with Cas9 mRNA and the Cas9 ribonucleoprotein (RNP). E) Frequency of indel formation in % (normalized to WT cells) in *HPRT* after cell transfection with RNAiMAX or DOPE-LNPs loaded with either Cas9 mRNA or RNP. F) Frequency of *HPRT* indel formation in % and G) cell viability of NHBE after transfection DOPE-LNPs loaded with total RNA concentrations between 0.5 and 10 µg/mL. Data are presented as mean ± SEM of at least three biologically replicates. * indicates statistically significant differences; *$p < 0.05$; **$p < 0.01$; ***$p < 0.001$.

versus RNP-treated NHBE (Fig. 2A, B). As expected, transfection with unmodified mRNA triggers the upregulation of genes that result in the suppression of viral genome replication such as *OASL*, chemokines (CXCL9, CXCL10 etc.) and interferons (Table S1). Interferons bind to foreign RNA and, thus, impair the binding of translation initiation factors, ultimately hampering RNA translation [37,38]. As expected, this was largely abolished when including pseudouridine modifications (Table S2). Both were further corroborated by Tmod, KEGG and

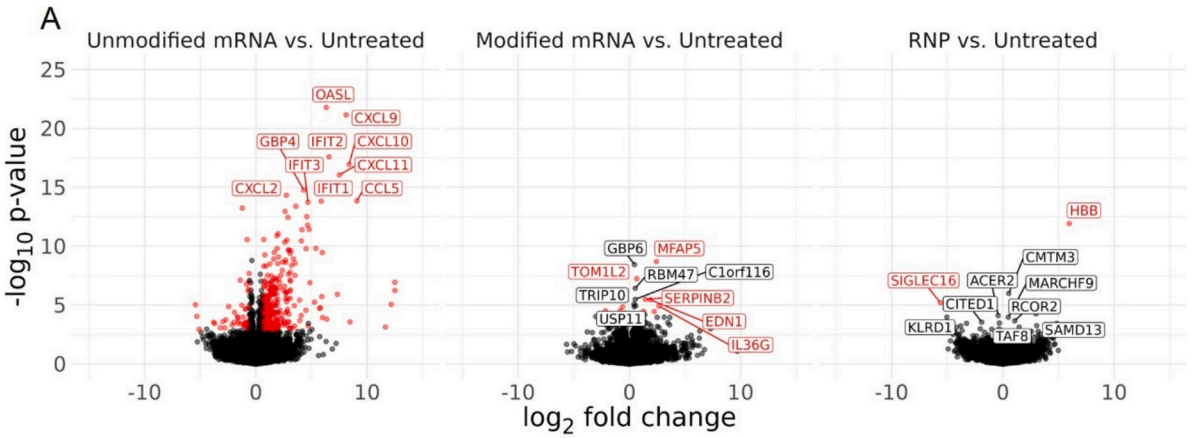

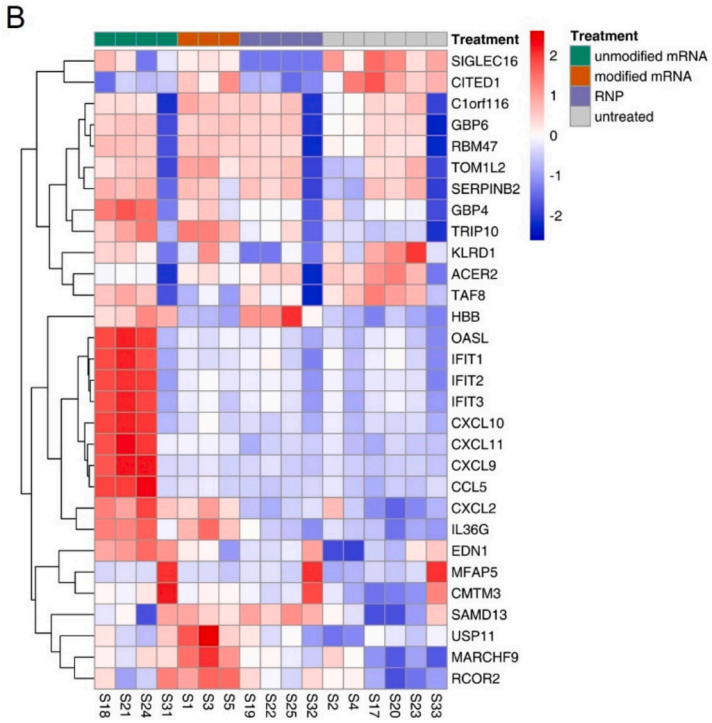

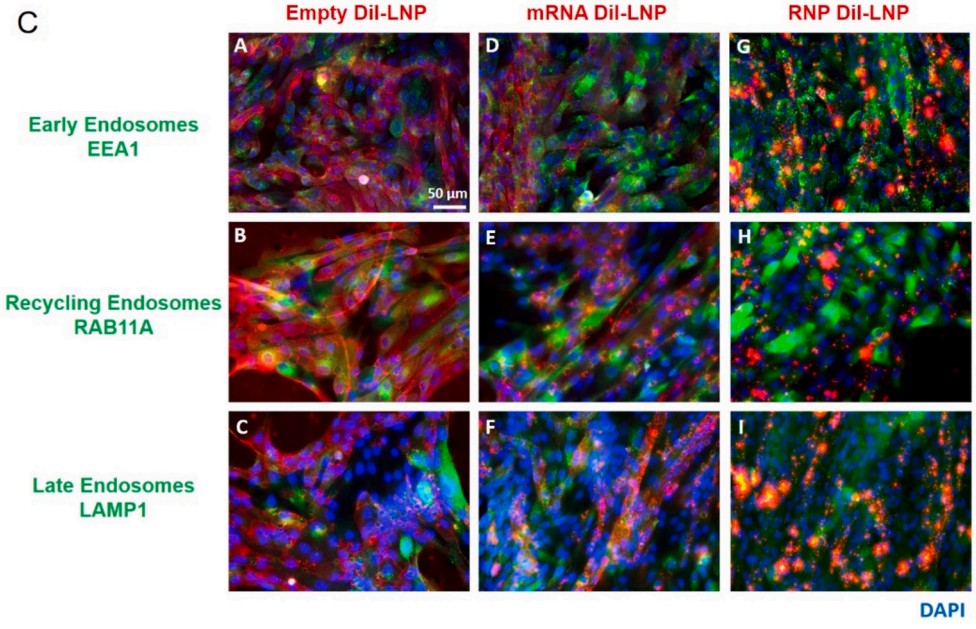

(caption on next page)

Fig. 2. A) Volcano plots for primary human bronchial epithelial cells (NHBE) transfected with unmodified and pseudouridine-modified Cas9 mRNA and Cas9 RNP, complexed with sgRNA targeting the *HPRT* gene, compared to untreated NHBE. Genes are colored by significance (FDR < 0.05 and fold change >1.5). B) Heatmap of the top 10 regulated genes for the unmodified Cas9 mRNA, pseudouridine-modified Cas9 mRNA, and Cas 9 RNP treated cells. C) Cas9 mRNA and RNP are differentially trafficked in NHBEs. NHBEs were treated with empty (A-C), mRNA-loaded (D—F) and RNP-loaded (G-I) DiI-LNPs and immunofluorescence staining of endosomal markers EEA1 (early endosome), RAB11A (recycling endosome) and LAMP1 (late endosome) was conducted. Scale bar represents 50 μm.

REACTOME pathway enrichment analysis. Those yielded main hits for pathways related to interferon responses and cytokine clusters as well as innate antiviral response for unmodified mRNA and leukocyte migration or protein synthesis pathways for cells transfected with modified mRNA (data not shown). For RNP treated NHBE, no enriched pathways were detected as well as no major differences in gene regulation were observed (Fig. 2, Table S3).

These results are noteworthy as we do not see improved gene editing when transfecting NHBE with modified or unmodified Cas9 mRNA (Fig. 1E, 3A) and only a slight increase with Cas9 RNP (Fig. 1E) indicating that innate immune responses are not the primary reason for the generally low editing efficacy.

Another bottleneck of hydrophilic and bulky therapeutics such as RNA is the endosomal maturation pathway subsequent to endosomal uptake and, thus, the challenge of endosomal escape which, however, is essential for functional effects [39,40]. Different factors including the size, zeta potential, cell type and carrier composition affect endosomal trafficking [41,42]. Also, some endosomes are processed towards exocytosis or maturation into lysosomes, which ultimately leads to degradation of the therapeutic cargo [43]. It is thus essential to unravel the intracellular trafficking to identify potential levers that could be used to increase the therapeutic index of genetic cargo. Hence, we determined the intracellular route of empty, mRNA or RNP-loaded DiI-labeled LNP and observed distinct compartmentalization (Fig. 2C). While mRNA-LNP predominantly colocalized in recycling and late endosomes, RNP-LNPs preferably colocalized with early and late endosomes. This may also explain the slightly higher editing efficacy observed with RNP-LNP (Fig. 1) as endosomal escape events occur more frequently from early endosomes [44,45].

2.3. Modifying sgRNA structure and sgRNA:mRNA ratios boosts gene editing efficacy

Next, we aimed to enhance the gene editing rates in NHBEs testing a

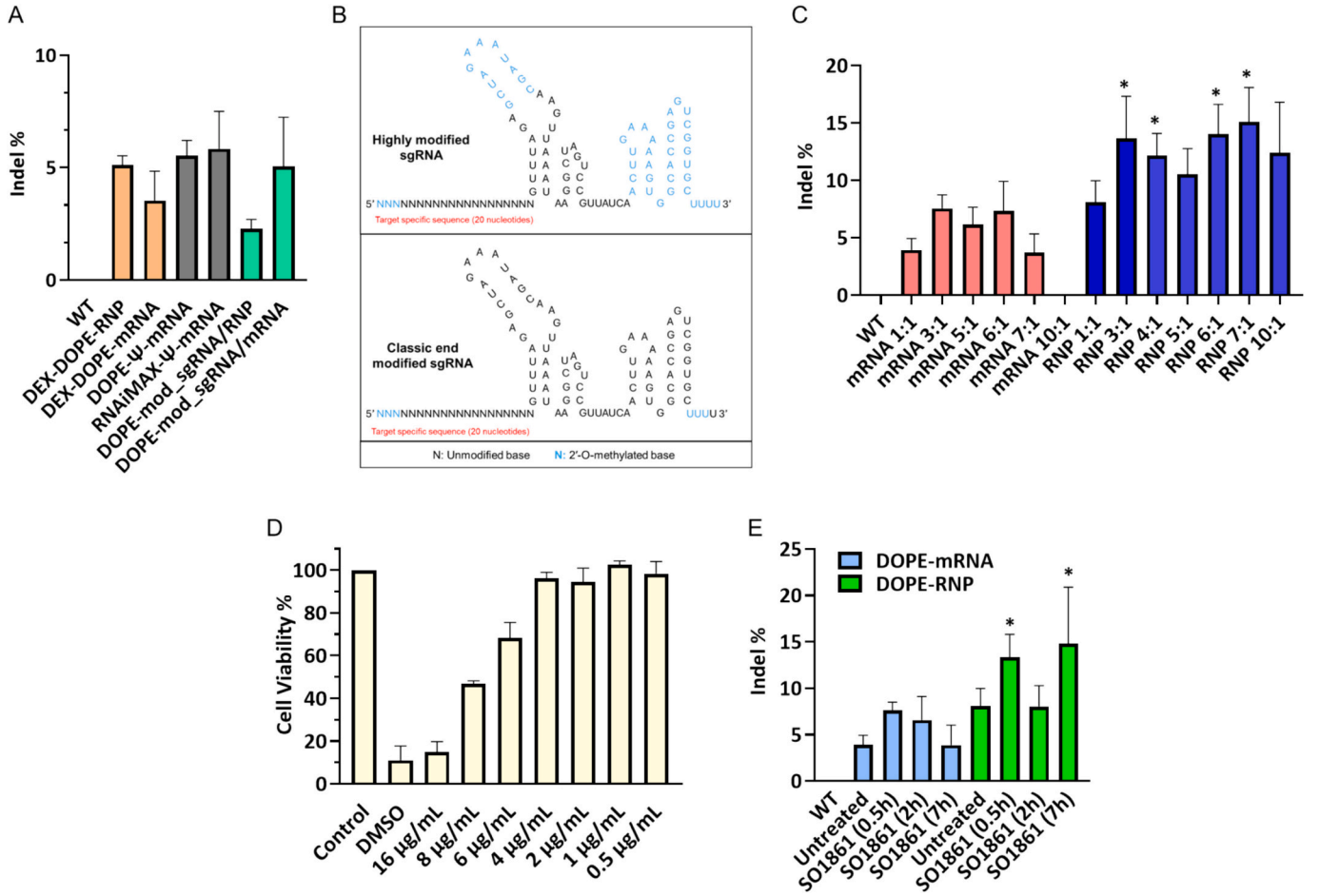

Fig. 3. A) Frequency of indel formation in the *HPRT* gene in % (normalized to wild-type (WT) cells) in NHBEs treated with mRNA or RNP-loaded LNPs or RNAiMAX in the presence or absence of dexamethasone (DEX), 100 % pseudouridinemodified Cas9 mRNA (ψ) and highly modified sgRNA (mod_sgRNA). B) 2′-*O*-methylation pattern of highly modified sgRNA (Mod_sgRNA) compared to classic end modified sgRNA. C) Frequency of *HPRT* indel formation in % (normalized to WT cells) after transfection of NHBEs with Cas9 mRNA or RNP-loaded LNPs at varying sgRNA/Cas9 ratios. D) Cell viability of NHBEs treated with increasing concentrations of SO1861 to determine the optimal dosage. E) Frequency of *HPRT* indel formation in % (normalized to WT cells) after transfection of NHBE cells with mRNA or RNP loaded LNPs (1:1 sgRNA:Cas9 ratio) and (pre-)treatment with SO1861 after different timepoints. Data are presented as mean ± SEM of at least three biological replicates. * indicates statistically significant differences over LNP-mRNA (1:1 sgRNA:mRNA and untreated with SO1861); *$p < 0.05$.

variety of approaches. First, we focused on strategies that mitigate the innate immune responses triggered by the RNA cargo. Considering the distinct pro-inflammatory effects of unmodified Cas9 mRNA, we tested if immunosuppressants like dexamethasone (DEX) would improve gene editing rates. However, as expected based on the bulk RNA-Seq data, no significant changes in indel percentage was observed (Fig. 3A). We also compared the editing efficacy of unmodified and 100 % pseudouridine (Ψ)-substituted mRNA. The latter reportedly increases mRNA stability and reduces its immunogenic potential and interferon levels [46]. However, again, no significant improvement was observed (Fig. 3A). Subsequently, we tested DOPE-LNPs with highly modified sgRNA (mod_sgRNA) which contains 2′-*O*-methylated bases throughout the stem-loop portion of the sgRNA sequence, which increases the stability of the loop and, thus, of the sgRNA overall, safeguarding it from degradation [47] (Fig. 3B). Classic sgRNAs are end-modified meaning that the last 3–4 bases on each end are 2′-*O*-methylated. Yet again, no increase in indel percentage was observed (Fig. 3A).

Notably, sgRNA is prone to faster degradation than Cas9 mRNA and RNP. To compensate for this, we next tested the impact of sgRNA:Cas9 ratios on indel formation. Indeed, increasing the sgRNA:Cas9 RNP ratios from 1:1 to 3:1, 6:1 and 7:1 yielded improved gene editing (~15 % indel formation) (Fig. 3C). Interestingly, for Cas9 mRNA, only moderate and statistically non-significant effects were detected. Similar to other data presented earlier, sgRNA:mRNA ratios 7:1 and 10:1 resulted in reduced editing likely due to the high total RNA concentrations and potential stimulating effects of the innate immune response hampering its protein translation.

Finally, we investigated the impact of the endosomal escape enhancer SO1861, a glycosylated triterpenoid, which facilitates endosomal escape of drugs into the cytosol [48]. Endosomal escape is a major bottleneck for genetic cargo with only <2 % reaching the cytosol [49] and, thus, being available for the actual gene editing. After identifying the maximal, non-toxic SO1861 dose (2 μg/mL), we added the enhancer at different time points after LNP treatment. While SO1861 had minor effects on mRNA-induced indel formation, it again significantly boosted RNP-induced indel formation from ~8 % to ~15 % (Fig. 3E).

Despite the possibility to increase gene editing efficacies after RNP delivery, the protein cannot be properly encapsulated in LNP [27] and RNP-loaded LNP hamper mucus penetration due to their large size [12]. Hence, we focused on mRNA cargo for the rest of the study.

2.4. Ionizable lipids significantly boost gene editing efficacy in NHBE

In previous work from our lab, we assessed the impact of ionizable lipids on the gene editing efficacy in primary epithelial cells including NHBE. We tested a range of ionizable lipids with pKas between 5.4 and 8.1 [27]. This screen identified ionizable lipids with a pKa ~7.1 as superior yielding gene editing rates of ~30 % (indel formation) in NHBE, outperforming other LNP formulations [27]. Since we failed to significantly increase the editing efficacy of mRNA-LNP in NHBE using the approaches detailed above, we continued our studies with this superior LNP formulation, termed LNP H. We also focus on mRNA-loaded LNP as RNP-loaded LNP have inferior mucus penetrating properties [12]. With LNP H, we tested the effect of combined strategies to enhance gene editing efficacies in normal and CF patient-derived NHBE. Importantly, functional mRNA expression in NHBE obtained from CF patients and non-CF donors do not differ following LNP transfection (Fig. 4A).

We first combined the most promising sgRNA:Cas9 mRNA 3:1 ratio with highly modified sgRNA and encapsulated it in LNP H (Fig. 4B). Transfecting NHBE with LNP H resulted in 30 % indel formation. Unexpectedly, however, increasing the sgRNA:Cas9 mRNA ratio to 3:1 did not further improve the gene editing rate. Interestingly, the combination with mod_sgRNA resulted in ~50 % indel formation which significantly outperformed all other treatments (Fig. 4B), while not impairing biocompatibility (Fig. 4C). These results clearly indicate distinct and still unknown effects of the LNP formulation itself. While it is clear that the ionizable lipid has a major impact, the exact mechanism remains ambiguous.

2.5. Gene editing rates drop dramatically in human 3D bronchial epithelial tissue models, but can be increased by pre-treatments with dornase alpha

The data presented so far have been generated in 2D cell monolayers. While this represents a critical initial test strategy, cell monolayers fail to reflect the native tissue architecture and lack the relevant biological barriers such as the mucus layer and beating cilia. Hence, to assess the gene editing efficacy of topically applied LNPs in a physiological environment, we utilized highly differentiated, human 3D bronchial epithelial models grown at the air-liquid interface (Fig. 5A) [50] which express all relevant biological barriers of human lungs. This includes a pseudostratified epithelium, beating cilia, and continuous mucus production and flow (Fig. 5A-C; supplementary video 1, Fig. S3) which is pivotal when striving for predictive preclinical data. While the functional characteristics of 3D bronchial epithelial models can vary between donors, our models consistently demonstrate excellent surface coverage with ciliated cells, a tight epithelial barrier evidenced by transepithelial electrical resistance (TEER) values within the literature-reported range of 150–600 $\Omega \cdot cm^2$ [51], and physiological ciliary beat frequencies (4–15 Hz [52,53]). Mucus production increases over time in a manner comparable to previously published data [54] (Fig. S3). While obtaining directly comparable human data on physiological mucin concentrations is challenging, analysis of bronchoalveolar lavage fluid (BALF) has shown MUC5AC levels, the predominant mucin in the lung, ranging from 4 to 12 ng/mL [55]. These values fall within the same order of magnitude as those observed in our models (~10–70 ng/mL, depending on cultivation time). It is important to note, however, that BALF typically underestimates true mucin concentrations due to sample dilution, processing-related degradation, and other limitations.

Following a thorough characterization of the bronchial epithelial models, we first compared functional GFP expression of LNP H and DOPE-LNP in normal bronchial epithelial models. While no GFP expression was observed following the topical application of DOPE-LNP, LNP H application resulted in functional GFP expression demonstrating its ability to effectively penetrate the mucus layer (Fig. 5D).

Next, we assessed the indel formation in normal bronchial epithelial models following topical LNP application. We initially tested LNP H loaded with 1:1 Cas9 mRNA:sgRNA at total RNA concentrations ranging from 1 to 12 μg. In line with the 2D data, increasing the total RNA amount did not further increase indel percentage in the 3D bronchial epithelial models and highest indel formation was obtained with 3 μg total RNA yielding ~7 % editing (Fig. 5E). For comparison, this formulation edited 30 % of the cells in a 2D monolayer (Fig. 4B).

We then generated bronchial tissue models using CF patient-derived NHBE which harbor the most common CFTR mutation F508del. As such, they develop key features of CF such as the significantly higher mucus viscosity. Impaired CFTR function in the 3D tissue models was verified by transepithelial ion transport measurements (Fig. 5F). The robustness of CFTR function was evident in the healthy 3D models, displaying a pronounced forskolin response, which was effectively suppressed by the specific CFTR inhibitor, CFTRinh-172, indicating functional CFTR activity (Fig. 5F). Notably, CF donor cultures exhibited expected characteristics, with minimal forskolin-induced responses and CFTRinh-172-sensitive currents. However, upon treatment with elexacaftor and tezacaftor (ET) for 24 h prior to measurement, followed by acute administration of ivacaftor (I), augmentation in these currents were observed (Fig. 6G-H). This observation suggests a functional rescue of CFTR chloride channel function following ETI treatment. The consistency of CFTR function across healthy, CF, and ETI-treated cultures aligns with anticipated outcomes. Following topical application of LNP H on 3D CF bronchial epithelial models, functional GFP expression was observed following LNP H application (Fig. 5D), although less

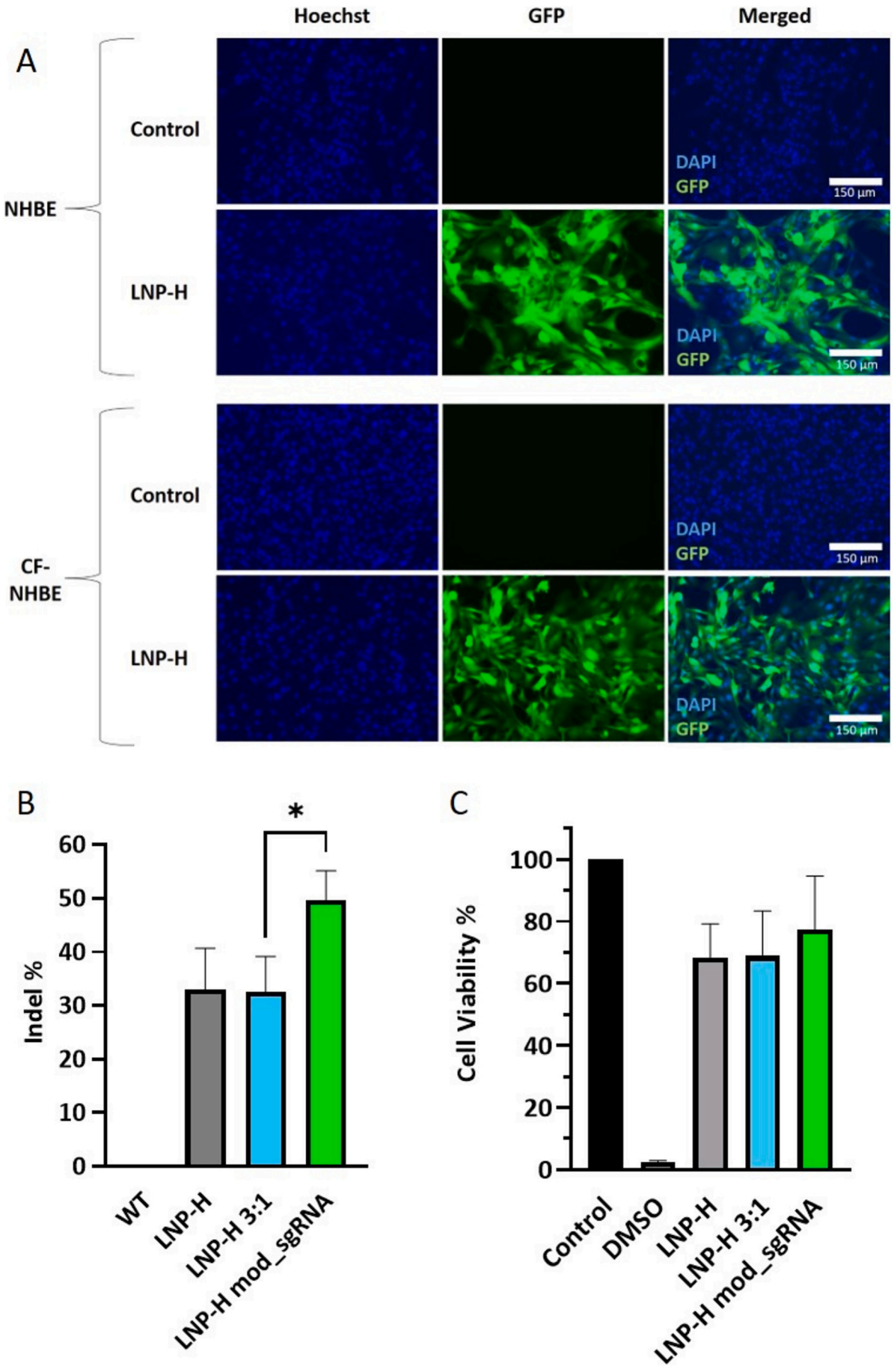

(caption on next page)

Fig. 4. A) Representative fluorescence microscopy images of function GFP mRNA expression in non-CF and CF patient-derived NHBEs (CF-NHBE) 24 h after transfection with LNP H. Scale bar = 150 μm. B) Frequency of indel formation in the *HPRT* gene in % (normalized to wild-type (WT) cells) after transfection of CF-NHBEs with LNP H loaded with 1:1 sgRNA:Cas9 mRNA (LNP H), 3:1 sgRNA:Cas9 mRNA (LNP H 3:1), and 1:1 highly modified sgRNA:Cas9 mRNA (LNP H mod_sgRNA). C) Cell viability of CF-NHBEs treated with LNP H, LNP H 3:1 and LNP H mod_sgRNA. Data are presented as mean ± SEM of at least three biological replicates. * indicates statistically significant differences over the indicated groups; *$p < 0.05$.

pronounced than in healthy bronchial epithelial models. The indel formation rates in CF bronchial epithelial models reached 5 % ± 2.14 which was slightly lower than in non-CF bronchial epithelial models (7 % ± 1.53, Fig. 5I). This drop in editing efficacy is likely attributed to increased mucus secretion and viscosity, resulting in fewer LNPs reaching the epithelial cells. Nevertheless, flow cytometry analysis of topically treated CF models demonstrated successful transfection of basal cells (TP63+; Fig. S5) within the bronchial epithelial model from which the bronchial epithelium regenerates. While the percentage of successfully transfected basal cells was low (~3 %) it represents an initial indication that topical LNP application may yield a durable and potentially curative effects. Single cell sequencing experiments will provide more detailed insights into the edited cells and potential downstream effects.

Next, we investigated the impact of a pretreatment with the clinically approved mucolytic drug Pulmozyme® (dornase alfa) prior to LNP application. Pulmozyme® is a nebulized DNAse I enzyme which reduces sputum viscoelasticity and is inhaled by CF patients twice per day as part of their mucus clearing routine. We topically pretreated 3D CF bronchial epithelial models with dornase alfa using a 15 U dose (0.015 mg at 1 mg/mL). 15 U was selected as a mid-low starting point as previous studies had looked at ranges from 3 U to 100 U and found no toxicity in cell culture [56]. Notably, the 4 h pretreated models achieved a significant improvement in editing, 9.32 ± 0.96 % indel formation, an almost 2-fold improvement in editing and the highest editing levels we observed in 3D CF bronchial epithelial models (Fig. 5J). Lastly, we sought to evaluate the dose-dependent response to DNAse I (Fig. 5K). Excitingly, editing increased with increasing doses of DNAse I in a dose-dependent manner and a high of 12.7 % editing was achieved with 60 U of DNAse I resembling a substantial improvement the gene editing levels. Interestingly, 60 U and 120 U performed very similarly indicating that an optimal dose is likely between 60 and 120 U. The established clinical mode of action of DNAse I is the degradation of microbial DNA which is highly abundant in CF patient mucus. As the 3D bronchial epithelial models are sterile, another mechanism seems to play a role. We therefore assessed the LNP diffusivity in mucin samples before and after DNAse I treatment. Most interestingly, the latter resulted in significantly enhanced LNP diffusivity (20.9×10^{-2} μm^2/s vs. 40.9×10^{-2} μm^2/s; Fig. S4, Supplementary Videos 2 and 3) indicating direct effects on mucins and/or the mucus hydrogel.

While the significant drop of editing rates in 3D tissue models compared to the 2D monolayer cultures was expected, editing rates of 5–10 % are potentially clinically relevant. In fact, a recent study demonstrated that editing rates of merely 1.27 % ± 0.29 % yielded a restoration of CFTR function of ~30 % compared to the wild-type [57]. Here, a viral vector has been employed which has distinct limitations including safety concerns, immunogenicity and high production costs. Other studies also reported that correcting between 5 %–10 % of the cells suffices to restore CFTR function [32,58].

Interestingly, Siegwart and colleagues [59] achieved <16 % editing in NHBE using the SORT LNP technology. With our approach, we yielded substantially higher editing levels (<50 % editing; Fig. 4) using comparable experimental settings. It should be noted, however, that Siegwart and colleagues reported homology-directed repair (HDR) rates, whereas we studied indel formation. The latter tends to yield higher editing efficacies than HDR.

Similar to our data, Siegwart and colleagues also reported a significant drop (to 4 %) of gene editing rates in 3D tissue models. Unfortunately, the exact nature and structure of their 3D cultures was not detailed rendering a direct comparison to our approach difficult. Here, we report 12.7 % editing with our combinatory DNAse I/ LNP delivery approach which significantly outperforms previous data. Another paper from the Siegwart lab [13] reported the topical application of dT Tomato mRNA-loaded LNP onto 3D bronchial epithelial models. While they demonstrated successful mRNA translation, no gene editing rates were reported.

To the best of our knowledge, these are the only studies were LNPs were topically administered onto human 3D bronchial epithelial models. Such studies, however, are pivotal to close a critical translational gap when moving from bench-to-bedside. While rodent models remain most commonly used for drug delivery studies to the lungs, it should be highlighted that rodents produce very little mucus and present a very different anatomical lung layout compared to humans [60]. Their poor predictive value has also been showcased by the failed Translate Bio clinical trial. Despite positive preclinical outcomes in mouse models and non-human primates, aerosolized LNPs failed to induce functional CFTR mRNA expression in CF patients. The authors noted that robust mRNA expression was not achieved in primary NHBE cells, highlighting a key limitation in their model selection [61]. 3D CF patient-derived models emulates the environment in a human respiratory tract more closely by expressing all relevant biological barriers rendering them critical tools when testing and developing drug delivery strategies yielding improved translation from bench-to-bedside. In vivo models, however, remain essential for other aspects of preclinical development such as biodistribution and toxicity studies.

2.6. LNP-mediated base editing of the disease-causing mutation $CFTR^{R1162X}$ using a novel adenine deaminase (ABE) base editor

Finally, we sought to provide the proof-of-concept for clinically relevant gene repair of a CF inducing point mutation using LNP H to deliver custom base editor mRNA. We selected the mutation $CFTR^{R1162X}$ which is a relatively common point mutation in CF patients and is theoretically amenable to adenine deaminase base editing. Adenine (ABE) base editors can repair the highest proportion of all single nucleotide mutations and are generally safer than cytosine base editors in terms of global transcriptome/genome effects [62–64].

First, we compared editing with two different ABEs in a HEK293 cell line that stably expresses a single copy of a CFTR gene fragment containing the R1162X mutation. This was selected as a starting point to demonstrate proof-of-concept editing in an 'easy to culture and transfect' immortalized cell line (Fig. 6A). The first ABE we tested was ABE8e-SpRY, which is a combination of a loosened PAM tolerance Cas9 variant [65] with the highly active "ABE8e" variant of the TadA deaminase [66]. The second ABE we compared was "ABE9p-SpRY" which is a novel combination of ABE TadA9 variants previously reported to produce high editing in plants [67]. We codon optimized it for mammalian expression by using the mammalian ABE8e architecture with these additional variants added and then combined it with the loosened protospacer adjacent motif (PAM) tolerance, SpRY, Cas9 variant. To the best of our knowledge this is the first report of successful editing in mammalian cells (Fig. 6B). Both ABE8e-SpRY and ABE9p-SpRY effectively corrected the $CFTR^{R1162X}$ site in HEK cells; 50 ± 3.06 % and 58 ± 8.54 % respectively. Although statistically not significant, there was a trend of higher editing rates with ABE9p-SpRY over ABE8e-SpRY.

Finally, ABE9p-SpRY was encapsulated in LNP H at a 1:1 ratio of mRNA:hypermodified sgRNA and 1 μg and 3 μg LNP H total was delivered to primary human nasal epithelial cells (Fig. 6B). CF nasal

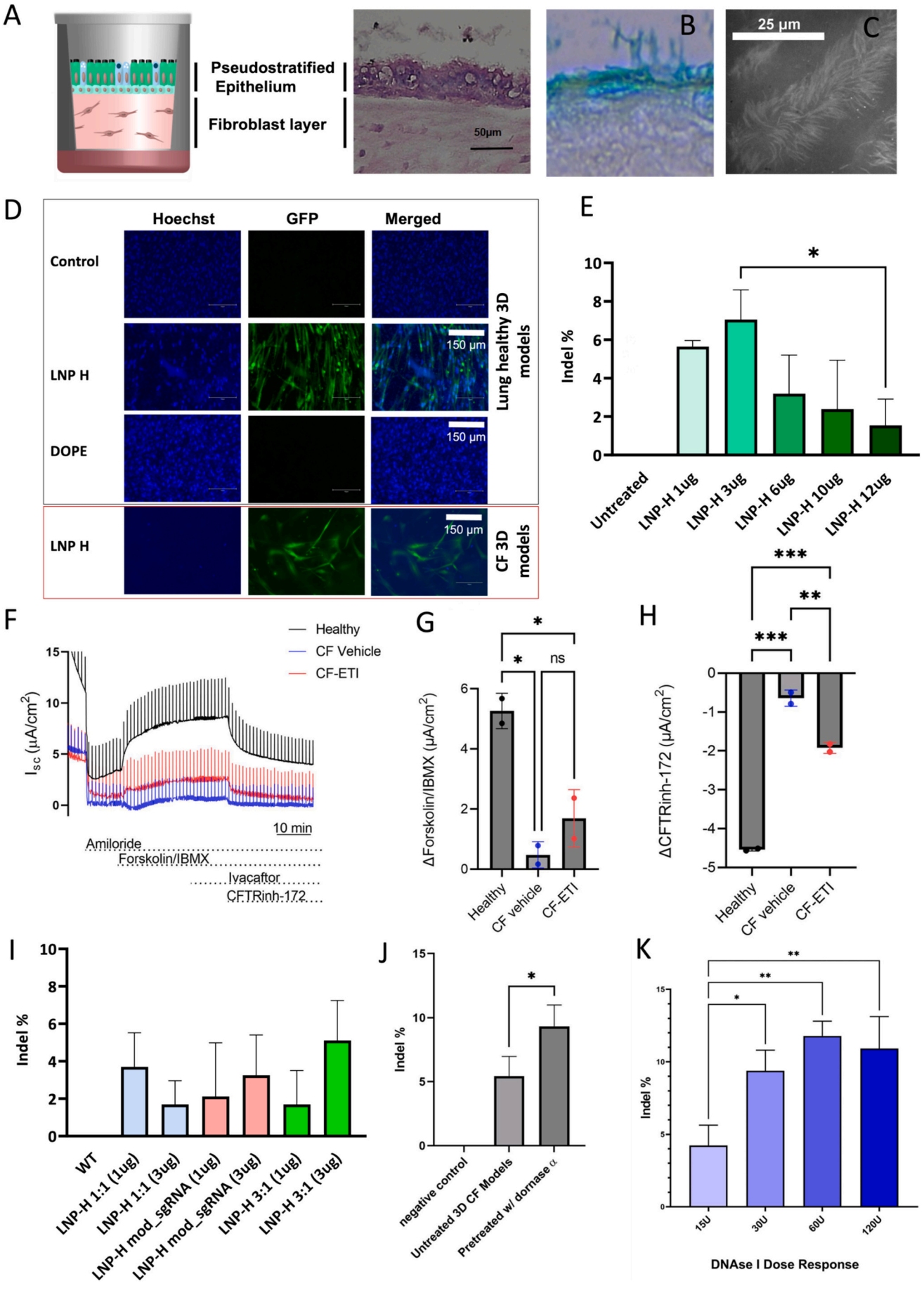

(caption on next page)

Fig. 5. A) Scheme and representative histological image of a human 3D bronchial epithelial model. B) Alcian blue staining shows the mucus layer on top of the cilia in 3D models. C) Close-up (100× objective) image of the cilia on top of the epithelial layer of the 3D models. D) Representative images showing functional GFP mRNA expression in normal and CF patient-derived 3D bronchial epithelial models following topical application of DOPE-LNP and LNP H. E) Frequency of indel formation in the *HPRT* gene in % (normalized to wild-type (WT) cells) in non-CF 3D bronchial epithelial models following topical application of Cas9 with LNP H (1:1 sgRNA/mRNA ratio) using increasing total mRNA concentrations. F—H) Administration of elexacaftor/tezacaftor/ivacaftor (ETI) effectively restores cystic fibrosis transmembrane conductance regulator (CFTR) functionality in 3D CF models. (F) Tracing of short-circuit transepithelial current (ISC) measurements in cultures from a healthy donor (black) and CF donor (blue -vehicle and red +ETI). Quantification of the effect of (G) cAMP activation (ΔForskolin/IBMX) and (H) CFTR inhibitor-172 (ΔCFTRinh-172) on normal and CF bronchial epithelial tissue models. I) Frequency of indel formation in % (normalized to WT cells) in 3D CF bronchial epithelial models following topical application of Cas9 with LNP H, LNP H mod_sgRNA, and LNP H 3:1 sgRNA/Cas9 at 1 μg and 3 μg total RNA concentrations. J) Frequency of indel formation in the *HPRT* gene in % (normalized to wild-type (WT) control models) after topical application of LNP H 3:1 sgRNA/Cas9 (3 μg total RNA) onto untreated and dornase α pretreated 3D CF models. K) Frequency of indel formation in the *HPRT* gene in % (normalized to wild-type (WT) control models) after topical application of LNP H 3:1 sgRNA/Cas9 (3 μg total RNA) onto untreated and DNAse I pretreated 3D CF models. Data are presented as mean ± SEM of at least three biological replicates. * indicates statistically significant differences over the indicated groups; *$p < 0.05$. (For interpretation of the references to colour in this figure legend, the reader is referred to the web version of this article.)

epithelial cells were heterozygous for the R1162X mutation and LNP H treatment resulted in a ~ 11.8 % editing at the target nucleotide with 3 μg LNP H (37.5 ± 1.32 % in untreated cells, 47.3 ± 0.95 % with 1 μg and 49.3 ± 1.76 % with 3 μg LNP H). Importantly, prior research by Geurts et al. 2020, on *CFTR*^{R1162X} yielded a ~ 8 % editing rate only after enrichment for positively transfected cells using plasmid DNA base editors delivered via electroporation to nasal organoids [10], the latter of which is not applicable in vivo. Future work will focus on the optimization of the mRNA architecture and the application in 3D tissue settings.

3. Conclusion

This study presents a systematic approach to optimize gene editing efficacies in 2D and 3D human lung models yielding clinically relevant in situ editing rates in 3D CF disease models following topical

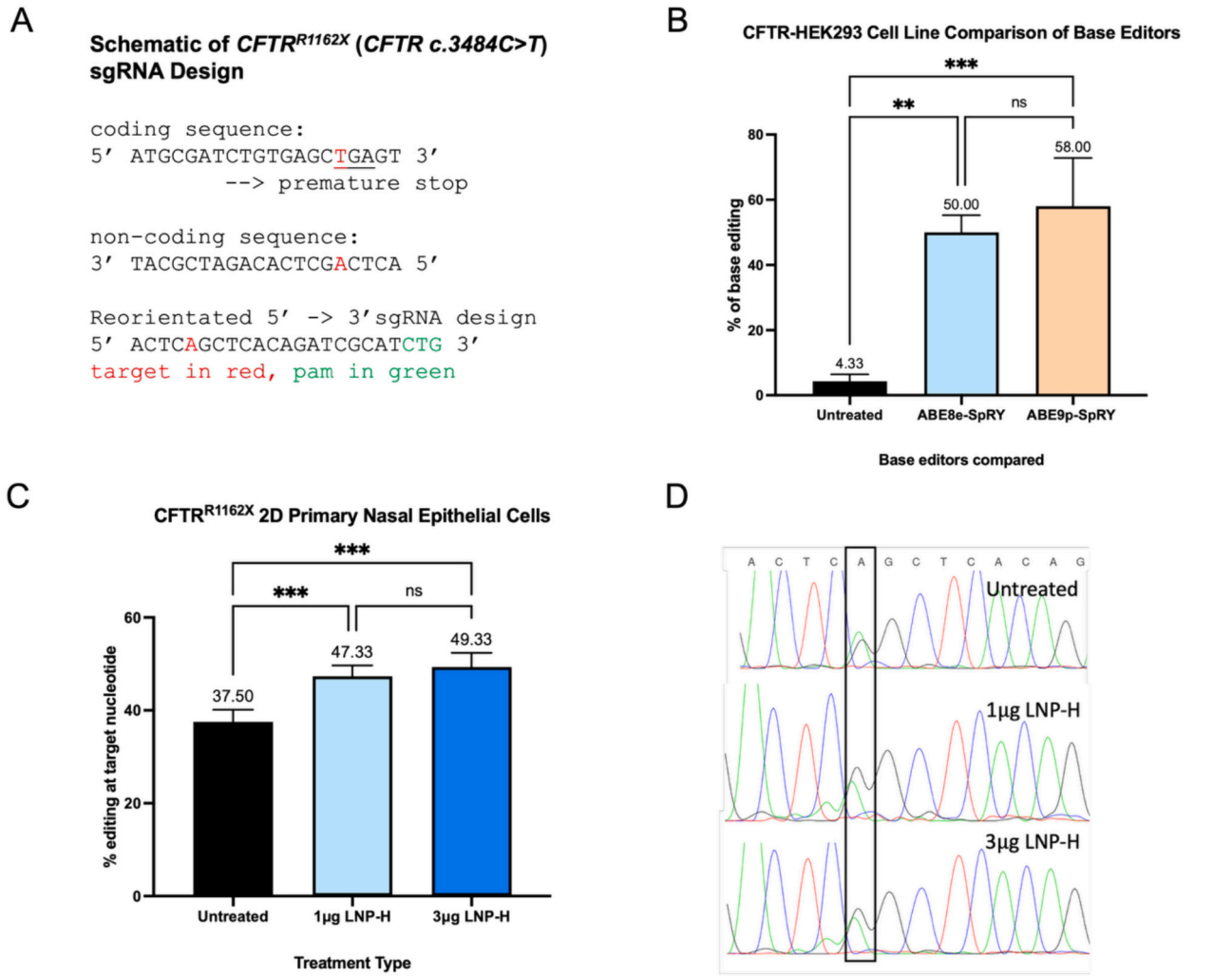

Fig. 6. A) Schematic of *CFTR*^{R1162X} loci and base editing sgRNA strategy. B) Percentage of adenine base editing at the target loci in immortalized HEK293 cells. Results analyzed by One-Way Anova. C) Evaluation of ABE9p-SpRY base editing in 2D primary nasal CF patient cells. Results analyzed by One-Way Anova. D) Representative Sanger sequencing results from *CFTR*^{R1162X} primary nasal cells untreated and treated with LNP H containing 1:1 ratio of hypermodified sgRNA and ABE9p-SpRY mRNA. Data is presented as mean ± SE of at least three biologically independent replicates. *Indicates statistically significant differences over the indicated groups; **$p < 0.01$, *** $p < 0.005$, ns denotes not significant.

application.

The importance of integrating human-based models in preclinical research has been recently showcased by the failure of a clinical trial conducted by Translate Bio. Here, aerosolized LNPs failed to induce functional CFTR mRNA expression in CF patients [61] despite positive preclinical data generated in HEK293 cells, mouse models and non-human primates. The authors stated, however, that they were unable to produce robust mRNA expression in primary human bronchial epithelial cells, which is a major red flag and highlights a key limitation in model choice. While in vivo models remain critical for certain aspects in preclinical development such as biodistribution and biocompatibility, the complementary use of human-based models of high clinical biomimicry, either freshly excised or bioengineered, is pivotal and can significantly enhance the translational value of preclinical research.

Our study demonstrates that optimizing the genetic cargo as well as the delivery vehicle is key when striving for clinically applicable treatment approaches. While the overall editing rate remains low, a growing body of literature shows the potential therapeutic benefits of correcting even a small fraction of cells – not only in CF. [68] In addition, optimizing the LNP with respect to their transmucosal diffusivity has great potential to even further increase its efficacy [12]. Finally, thinking about a clinical application, combinations with mucolytics such as dornase alfa or novel mucus reducing agents [69,70] may further improve the correction rates and should be investigated Eventually, successful transmucosal delivery will offer great therapeutic opportunities not only for CF, but also other genetic lung diseases such as primary ciliary dyskinesias, or genetically determined interstitial lung diseases such as surfactant protein B or C deficiencies. Another critical aspect that requires attention in future studies is the aerodynamic compatibility of the LNPs which is mandatory when striving for local lung administration. Different approaches are currently explored such as spray-drying LNPs [71] or harnessing LNP-"friendly" inhalers or nebulizers [72] as well as novel aerosolization technologies to reduce shear stress and, thus, preserve the physicochemical properties and biological activity of LNP-mRNA [73].

4. Methods

4.1. Materials and primary cells

Single guide RNAs (sgRNAs; HPRT: AATTATGGGGATTACTAGGA, CFTR: ACTCAGCTCACAGATCGCATCAA), GFP mRNA, Cas9 protein nuclease, PCR primers, and probes, as well as PrimeTime qPCR mix, were purchased from IDT (San Jose, CA, USA). The Cas9 mRNA was purchased from TriLink Biotechnologies (San Diego, CA, USA). PneumaCult™-Ex Plus medium and PneumaCult™-ALI medium were obtained from StemCell (Vancouver, BC, Canada). Dulbecco's Modified Eagle's Medium (DMEM), fetal bovine serum, and penicillin were purchased from Fisher Scientific (Mississauga, ON, Canada). Apolipoprotein 4 (ApoE4) was obtained from Peprotech (Rocky Hill, NJ, USA). Healthy and cystic fibrosis primary human bronchial epithelial cells (NHBE) were purchased from Epithelix (Geneva, Switzerland), ATCC (Manassas, Virginia, USA), and McGill University (Montreal, Quebec, Canada). NHBE cells were cultured in PneumaCult™-Ex Plus media for 2D culturing or in PneumaCult™-ALI medium for 3D model culturing. All cells were maintained at 37 °C in a humidified atmosphere containing 5 % CO_2.

4.2. Lipid Nanoparticle (LNP) preparation and loading

To generate LNPs, a lipid mixture dissolved in ethanol at appropriate ratios to achieve a final concentration of 10 mM lipid was injected with an aqueous phase containing Cas9 mRNA and HPRT sgRNA through a T-junction at a 3:1 volume ratio and an amine-to-phosphate (N/P) ratio of 6.87. Flow rates were adjusted to 5 mL/min for the lipid-phase syringe and 15 mL/min for the aqueous-phase syringe containing the RNA dissolved in 25 mM sodium acetate (pH 4), resulting in an output flow rate of 20 mL/min. The resulting formulation was dialyzed in Spectra/Por 2 12–14kD molecular weight cut-off (MWCO) dialysis tubing (Spectrum Laboratories) against 1000-fold volume of phosphate-buffered saline (pH 7.4) overnight at room temperature to remove the ethanol. The formulations were then sterile-filtered and concentrated to target nucleic acid concentrations using 10 kDa Amicon filters (Sigma-Aldrich).

For RNP loading, a benchtop mixing approach was utilized. Empty LNPs were prepared as described above followed by cargo loading [74]. Here, RNP complexes were formed by combining sgRNA with the Cas9 protein at 1:1 equimolar ratio in 10 mM Tris, 0.1 mM ethylenediaminetetraacetic acid (EDTA) buffer at pH 7.5 to a final working concentration of 25 μM, followed by incubation at room temperature for 5 min. For LNP-RNP complexation, 100 nM RNP (pH 7.5) was mixed with LNPs at L/R 500 (LNPs amounts with initial stock of 3 mM; 0.053 μmol (L/R 500)). For other sgRNA to Cas9 protein molar ratios (3:1–10:1), the sgRNA amount was adjusted accordingly. For mRNA encapsulation, sgRNA and Cas9 mRNA were mixed with a 1:1 equimolar ratio to a 10 μg/mL final working concentration.

The final lipid concentration was determined using a Total Cholesterol Assay kit (Wako Chemicals, Richmond, VA, USA). A typical LNP formulation would consist of ionizable cationic lipid, phospholipid (DOPE (1,2-di-(9Z-octadecenoyl)-*sn*-glycero-3-phosphoethanolamin), DSPC (1,2-distearoyl-sn-glycero-3-phosphocholine), or DOPC (1,2-Di-(9Z-octadecenoyl)-*sn*-glycero-3-phosphocholin)), cholesterol, and PEG-lipid at 50/10/38.5/1.5 mol%, respectively. For systems incorporating fluorescent labels, DiI-C18 (Invitrogen, Carlsbad, CA) was added at 0.2 mol% instead of cholesterol. All ionizable lipids except for MC3 were proprietary cationic lipids synthesized by NanoVation Therapeutics. After adding the RNP to the lipids, which were dispersed in a pH 4 acetate buffer, a neutral buffer or cell culture medium was swiftly added to adjust the formulation to pH 7.4. For treatments involving dexamethasone (DEX), NHBEs were pretreated with 100 nM DEX (40 ng/mL) in Pneumacult Ex-Plus media for 2 h at 37 °C with 5 % CO_2 followed by the addition of LNP-mRNA or LNP-RNP. 24 h later, the media was changed and cells were kept for another 24 h. SO1861 was isolated from *Saponaria officinalis* L. as described elsewhere [75]. 2 μg/mL SO1861 was added to LNP-mRNA or LNP-RNP-treated NHBEs at 0.5, 2, and 7 h, respectively. Notably, previous work from our lab has determined critical design parameter for LNPs aiming for superior mucus penetrating properties by modulating PEG levels and compositions [12]. These PEG modifications have not been included in this study, where we focused on strategies to optimize the gene editing efficacies.

4.3. LNP characterization

For sizing and determining the ζ potential of LNP formulations, the samples were diluted in 1 mL of cell culture media (pH 7.4). The number mean (d.nm), polydispersity index (PDI), and ζ potential were then measured using a Zetasizer Nano ZS instrument (Malvern Panalytical, St. Lauren, Canada).

To determine the encapsulation efficiency (EE%) of RNP and mRNA, the Quant-iT Ribogreen fluorescence assay was conducted as per the manufacturer's instructions. In brief, the loaded LNPs were diluted in sodium acetate buffer (pH 4.0) containing Ribogreen, with or without 0.5 % (*w/v*) Triton X-100 in Tris-EDTA buffer. Fluorescence was measured at $\lambda ex = 500$ nm and $\lambda em = 525$ nm. The total RNP and mRNA content was determined from a standard curve, and EE% was calculated by comparing RNP and mRNA concentrations with and without Triton X-100. A summary of the LNP characteristics used in this study is provided in Table 1.

Table 1
Lipid nanoparticle (LNP) size, polydispersity index, encapsulation efficiency and zeta potential.

LNP	Size (polydispersity index)	Encapsulation efficiency [%]	Zeta potential (pH 7)
Unloaded DSPC-LNP	35 nm (0.15–0.17)	–	–
Unloaded DOPC-LNP	38 nm (0.19–0.25)	–	–
Unloaded DOPE-LNP	38 nm (0.16–0.25)	–	–
DSPC-mRNA	55 nm (0.17–0.25)	<90 %	−2.13 ± 0.3 mV
DOPC-mRNA	51 nm (0.16–0.21)	<90 %	−2.63 ± 0.5 mV
DOPE-mRNA	42 nm (0.19–0.27)	~31 % (per bench-top mixing to allow head-to-head comparison with RNP-loaded LNP)	−10 ± 5.0 mV
DOPE-RNP	279 nm (0.40–0.75)	~18 %	−1.8 ± 1.0 mV
LNP-H	46 nm (0.10)	<90 %	- 2 ± 0.1 mV

4.4. Luciferase reporter assay

NHBE transfection was semi-quantified using the luciferase assay (Promega, Madison, Wisconsin, United States). 1 μg/mL luciferase mRNA was loaded onto LNPs, being composed of DOPC, DSPC and DOPE as helper lipids. Subsequently, cell culture media spiked with 1 μg/mL ApoE4 were added to a final volume of 1 mL, followed by 10 min of incubation at room temperature. The uptake efficiency was then tested in the presence or absence of ApoE. After 24 h of treatment, the cells were processed according to the manufacturer's instructions (Promega, Madison, Wisconsin, United States). Relative luminescence activity was quantified using a Biotek Synergy 2 Plate Reader.

4.5. Transfection efficacy

Functional mRNA expression of GFP-mRNA loaded LNPs was visualized by EVOS M5000 Imaging System (Thermo Fisher Scientific, Burlington, ON, Canada). NHBE cells were seeded in 12-well plate at 100,000 cells/well overnight at 37 °C and 5 % CO_2 and then treated with LNPs loaded with GFP-mRNA (1 μg/mL). After 24 h, the medium was removed, and cells were washed with PBS. The nuclei were stained using Hoechst 33342 Solution (Thermo Fisher Scientific CatNr. 62249, 1:2000 dilution) and functional GFP expression was imaged using an EVOS M5000 Imaging System (Thermo Fisher Scientific, Burlington, ON, Canada).

4.6. Intracellular trafficking

To investigate the intracellular localization of LNP within endosomes, NHBEs were treated with either empty DiI-labeled LNPs, or LNPs loaded with mRNA or RNP over 12 h. Subsequently, the cells were fixed using a 4 % formaldehyde solution, followed by PBS washes and permeabilization with 0.5 % Triton-X-100 (VWR, CatNr. 97063–864). Blocking was accomplished using normal goat serum (ThermoFisher Scientific, CatNr. PCN5000), diluted 1:20 in PBS, for 30 min at room temperature. Primary antibodies targeting EEA1 (Invitrogen, CatNr. 14–9114-82, dilution 1:1000), RAB11A (Invitrogen, CatNr. 71–5300, dilution 1:350), and LAMP1 (Abcam, CatNr. ab25630, dilution 1:1000) were applied to the cells overnight at 4 °C. Following incubation, NHBEs were washed and exposed to corresponding Alexa Fluor 488-conjugated secondary antibodies (Abcam CatNr. ab150113 and ab150077, dilution 1:400). After air-drying, NHBEs were mounted using Fluoroshield with DAPI overnight at 4 °C.

4.7. MTT cell viability assay

Cell viability was measured using a 3-(4,5-dimethylthiazol-2-yl)-2,5-diphenyl tetrazolium bromide (MTT) assay. Here, 1×10^4 cells NHBE were seeded in 96-well culture plates, respectively, and cultivated until ~70 % confluency. Subsequently, the cells were treated with the different LNP formulations at 37 °C for 48 h. Afterwards, 10 μL of a 5 mg/mL MTT solution was added to each well, and the plates were incubated for 4 h. The MTT formazan crystals were then dissolved in 50 μL of dimethyl sulfoxide (DMSO). Finally, the absorbance was measured in a microplate reader (BioTekuQuant, Winooski, VT, USA).

4.8. Bulk RNA-Seq

NHBEs were seeded in a 6-well plate at 300,000 cells/well overnight at 37 °C and 5 % CO_2 and subsequently treated with DOPE-LNP loaded with Cas9 mRNA/sgRNA or RNP (1:1 ratio). Untreated NHBE served as control. After 4 h, the total RNA was isolated using the Invitrogen PureLink™ RNA Mini Kit (ThermoFisher, Burnaby, BC, Canada) according to the manufacturer's protocol.

Sample quality control was performed using the Agilent 2100 Bioanalyzer or the Agilent 4200 TapeStation. Qualifying samples were then prepped following the standard protocol for the Illumina Stranded mRNA prep (Illumina). Sequencing was performed on the Illumina NextSeq2000 with Paired End 59 bp × 59 bp reads. Sequencing data was demultiplexed using Illumina's BCL Convert. De-multiplexed reads were aligned to *H. sapiens* version GRCh38, p7 with GENCODE annotation v. 25 using the STAR aligner v. 2.7.11a [76]. Read counts were extracted using featureCounts [77] implemented in package subread v. 2.0.3. Differential expression analysis was performed using the R package DESeq2, v. 1.38.0. Gene set enrichment was performed with the CERNO algorithm implemented in the R package tmod [78], v. 0.51.3. The RNA-Seq data have been deposited in GEO, accession GSE287215 (for review, go to https://www.ncbi.nlm.nih.gov/geo/query/acc.cgi?acc=GSE287215 and enter token cvuhkmeiltqzvwz).

4.9. Quantification of genome editing using PrimeTime qPCR

To determine gene editing rates, 1×10^5 NHBE cells were plated in 12-well plates and incubated overnight at 37 °C with 5 % CO_2. Subsequently, the cells were transfected with LNPs encapsulating *HPRT* sgRNA and Cas9, delivered either as mRNA or RNP, following a previously described LNP preparation and loading protocol [27]. After 48 h, genomic DNA was extracted using the Qiagen DNeasy Blood&Tissue Kit (Toronto, ON, Canada) following the manufacturer's instructions. The genomic DNA was then amplified by PCR using 10 μM HPRT primers, 5 μM of reference and drop-off probes, PrimeTime master mix, and water to a final reaction volume of 20 μL. The drop-off probe was specifically designed to bind the wild-type template and target the predicted cut sites. The PCR program included an initial denaturation step at 95 °C for 3 min, followed by 40 cycles of 95 °C for 15 s, and annealing/extension at 60 °C for 1 min. The gene editing efficiency (indel %) of the formulations was determined by calculating the ΔΔCT values of drop-off and reference probes and normalizing them to the wild-type cells.

4.10. Generation and treatment of 3D bronchial epithelial models

3D bronchial epithelial tissue models were generated according to previously published procedures [50]. Briefly, 6.43×10^4 normal human lung fibroblasts were embedded in a matrix consisting of fetal bovine serum and bovine collagen I (PureCol, Advanced BioMatrix, San Diego, USA) at a neutral pH. After solidification, primary human NHBEs from non-CF donors and CF patients harboring the *ΔF508 CFTR*

mutation (0.9×10^6 per model) were seeded on top. After 24 h, the models were lifted to the air–liquid interface and further cultivated until day 21 with media changes every other day. Starting on day 14, the models were washed with PBS every second day to remove the mucus. For histological and Alcian blue staining, the bronchial epithelial models were snap frozen using liquid nitrogen, cryosectioned and subsequently stained with hematoxylin and eosin or Alcian blue (Sigma-Aldrich, Oakville, Ontario, Canada) according to standard procedures. To visualize the cilia beating of the bronchial epithelial models, the models were stained overnight with CellMask™ Plasma Membrane Stain (C10046, ThermoFisher, Burnaby, BC, Canada). Subsequently, the live movement of beating cilia was recorded at 30 frames per second using the PerkinElmer VoX Spinning Disk fluorescence microscope (PerkinElmer, Woodbridge, ON, Canada) equipped with 100× objective, a high-speed Hamamatsu 9100–02 CCD camera and a thermoplate heated to 37 °C.

To determine the in situ gene editing rates in the tissue models, 15 μL LNPs loaded with Cas9 mRNA/sgRNA were topically applied at day 21 of tissue culture. After 48 h, the genomic DNA was isolated and editing rates were determined as detailed above. To visualize functional mRNA expression, 15 μL of each LNP formulation was applied topically to the models followed by a 24 h incubation at 37 °C with 5 % CO2. Subsequently, the models were maintained in an upright position and functional GFP expression was visualized using the inverted EVOS M5000 Imaging System (Thermo Fisher Scientific, Burlington, ON, Canada). To determine which cells were transfected within the 3D bronchial epithelial models, flow cytometry analysis was performed. 48 h after topical application of GFP mRNA-loaded LNP H, the models were dissociated according to established protocols and subjected to flow cytometry. In brief, TrypLE was added to the cells and incubated for 10 min at 37 °C with 5 % CO_2 followed by gently pipetting the cells up and down. The cells were then transferred into an Eppendorf tube and the mixture was incubated at 37 °C with agitation for 15 min. Subsequently, the cells were further dissociated using a 22-gauge syringe. Stop media (DMEM + FBS) was then added to neutralize the TrypLE. The cell suspension was passed through a 100 μm cell strainer and washed with PBS. Finally, the suspension was centrifuged at 300 ×*g* for 5 min, and the supernatant was carefully aspirated. The cells were sorted for GFP expression and TP63 as a stem cell marker (Novus Biologics, NBP3-08736AF594) using a Cytek Aurora™ CS System (Cytek Biosciences).

To evaluate the effects of dornase alpha as a pre-treatment to CF 3D models, models were grown as described above. After 21 days all models were washed with PBS as done in all prior experiments. 24 h later (day 22), models were either treated with dornase alpha (15 μL for a total of 15 U) or left untreated. 4 h later, the models were treated with 15 μL of LNP H. After 48 h, the genomic DNA was isolated and editing rates were determined as detailed above. DNase I dose dependent gene editing responses were compared using commercially available DNAse I lyophilized powder (Luna Nanotech, Markham, Ont. Canada, #GDN-550) and resuspended at 120 U, 60 U, 30 U and 15 U total doses in 15 μL dilutions in PBS, made fresh prior to treatment. All concentrations were treated on 21-day old CF lung models for 4 h prior to LNP H transfection. All other experimental parameters were conducted as previously described.

4.11. Preparation of mucin hydrogels and Multiple Particle Tracking (MPT)

Native mucin from bovine submaxillary glands (Sigma-Aldrich, St. Louis, MO, USA) was dissolved in calcium- and magnesium-free DPBS, gently mixed at room temperature for 1 h, then incubated overnight at 4 °C for full hydration. A 2 % (*w/v*) mucin concentration was used to mimic healthy mucus. For DNase treatment, 200 μL of hydrogel was incubated with 60 units of DNase I for 4 h at 37 °C; controls received PBS. To assess LNP diffusivity, LNPs were added to the hydrogel (≤0.2 % final volume), mounted on slides with coverslips, and imaged using a PerkinElmer VoX spinning disk confocal microscope (63× glycerol-immersion objective, Hamamatsu 9100–02 CCD camera) at 37 °C according to [12]. Time-lapse videos (10 FPS, 30 s) tracked ≥10,000 LNPs per condition. Particle tracking was done with NanoTrackJ in ImageJ (v1.53k), using "Spot Assistant" for parameter optimization. Only particles with ≥10 steps per track were analyzed. Diffusion coefficients were calculated via the plugin's covariance-based method.

4.12. Short-circuit (I_{sc}) measurements in Ussing chambers

CF bronchial epithelial models underwent treatment with elexacaftor (3 μM, Selleck Chemicals, CatNr. 8851) and tezacaftor (2 μM, Selleck Chemicals, CatNr. S7059) or DMSO (Sigma Aldrich, CatNr. 472301), as vehicle control for 24 h prior to Ussing chamber analysis. Ivacaftor (2.5 μM, Selleck Chemicals, CatNr. S1144) was added acutely during measurements in cultures pre-treated with ET. Isc was measured in symmetric chloride conditions as previously described [79].

4.13. Base editing of $CFTR^{R1162X}$ in HEK cells and CF patient-derived cells

HEK293 cells were cultured in high glucose Dulbecco's Modified Eagle's Medium (DMEM) (VWR Cat. #VWRL0102–0500) supplemented with 10 % Fetal Bovine Serum (FBS), 1 % L-glutamine (Gibco™ Cat# 25030081) and 1 % Antibiotic-Antimycotic (100×) (Gibco™ Cat#15240062). $CFTR^{R1162X}$ stable cell lines were generated using the Flp—In™ system and the Flp—In™ HEK293 cell line (Invitrogen™) according to manufacturer's specifications. Flp—In™ 293 cells were cultured in HEK293 media according to the manufacturer's specifications.

4.5×10^5 HEK293 cells were plated in 12 well plates pre-treated with Poly-D-lysine (Gibco™ Cat#A3890401) and incubated overnight at 37 °C with 5 % CO_2. Media used for seeding experimental plates was deficient of antibiotics. Cells were transfected with 4 μg total RNA (at a ratio of 1:1 sgRNA to mRNA) using Lipofectamine™ RNAimax (Thermo Fisher Scientific Burlington, ON, Canada). After 48 h, genomic DNA was extracted using the Qiagen DNeasy Blood&Tissue Kit (Toronto, ON, Canada) following the manufacturer's instructions. PCR was used to amplify the target loci and samples were sent for Sanger sequencing conducted by the Sequencing and Bioinformatics Consortium (SBC), Vancouver, BC.

CRISPR/Cas9 base editor mRNA was made using in vitro transcription (IVT) from custom cloned base editor vectors. Vector sequences confirmed via Nanopore sequencing conducted by Plamsidsaurus©, San Francisco, California, USA. ABE8e-spRY base editor sequence was copied directly from [66]. ABE9p-spRY was taken from TadA9 variants used in Yan et al. 2021 [67] and codon optimized for mammalian expression. The base editors used in this study were cloned using golden gate assembly to make the initial SpRY-ABE8e and the novel base editor SpRY-ABE9p (TadA8e with V82S/Q154R mutations). Briefly, SpRY-Cas9 was PCR-amplified from the SpRY-ABE8e (Addgene #185671) with primers containing PaqCI restriction sites. SpRY-Cas9 was then cloned into a cloning vector containing PaqCI sites and Esp3I sites. TadA8e deaminase and variants were synthesized by TwistBioscience and cloned into the vector containing SpRY-Cas9 using Esp3I. This plasmid was then used as the template for PCR-amplification to install *Bsm*BI restriction sites on the base editor and cloned using golden gate assembly into a mRNA expression vector containing a T7 promotor, the Pfizer 5′ and 3' UTRs, and a poly-A-tail (vector kindly gifted by the UBC RNACore). Highly modified sgRNA was ordered from IDT, Coralville, Iowa, USA.

For $CFTR^{R1162X}$ primary cell experiments, $CFTR^{R1162X}$ nasal epithelial cells were obtained from the Charité Universitätsmedizin, Berlin Germany (written consent obtained, ethics vote EA2/016/18). 1×10^5 nasal epithelial cells were plated in 12-well plates and incubated overnight at 37 °C with 5 % CO_2. Subsequently, the cells were transfected

with mRNA-loaded LNPs using the aforementioned protocol. After 48 h, genomic DNA was extracted using the Qiagen DNeasy Blood&Tissue Kit (Toronto, ON, Canada) following the manufacturer's instructions. PCR was used to amplify the target loci and samples were sent for Sanger sequencing conducted by the Sequencing and Bioinformatics Consortium (SBC), Vancouver, BC.

4.14. Statistical analysis

Statistical analysis was performed using Prism Graphed 9.6 software (San Diego, CA, USA). Each experiment was performed at least in triplicate, and results are shown as mean ± standard error (SE). The statistical significance was determined using one-way analysis of variance (ANOVA) followed by Tukey or Fisher's LSD multiple comparison test. *p*-Values ≤ 0.05 were considered statistically significant. For base-editing experiments, the statistical significance was assessed with a two-way multiple comparison ANOVA.

Supplementary data to this article can be found online at https://doi.org/10.1016/j.jconrel.2025.114053.

CRediT authorship contribution statement

Belal Tafech: Writing – review & editing, Writing – original draft, Visualization, Validation, Methodology, Investigation, Data curation. **Tiffany Carlaw:** Writing – review & editing, Writing – original draft, Methodology, Investigation. **Gaurav Sadhnani:** Investigation, Formal analysis, Data curation. **Konrad Schmidt:** Investigation, Formal analysis, Data curation. **Tessa Morin:** Methodology, Investigation. **Jerry Leung:** Methodology, Investigation. **January Weiner:** Visualization, Software, Investigation, Data curation. **Kevin An:** Methodology, Investigation. **Anita Balázs:** Methodology, Investigation. **Colin Ross:** Supervision, Project administration. **Dieter Beule:** Methodology, Formal analysis. **Marcus A. Mall:** Supervision, Methodology, Investigation. **Hendrik Fuchs:** Methodology, Investigation. **Jay Kulkarni:** Methodology, Investigation. **Pieter R. Cullis:** Supervision, Methodology, Investigation. **Sarah Hedtrich:** Writing – review & editing, Writing – original draft, Supervision, Resources, Project administration, Methodology, Funding acquisition, Formal analysis, Data curation, Conceptualization.

Declaration of competing interest

PRC has a financial interest in Acuitas Therapeutics and NanoVation Therapeutics as well as being Chair of NanoVation Therapeutics. KA and JK are employees of NanoVation Tx and JK is a co-founder. MAM reports grants and contracts from the German Research Foundation (DFG), the German Federal Ministry of Education and Research (BMBF), Boehringer Ingelheim, Enterprise Therapeutics and Vertex Pharmaceuticals with payments made to the institution; personal fees for advisory board participation or consulting from Boehringer Ingelheim, Enterprise Therapeutics, Kither Biotech, Splisense, Vertex Pharmaceuticals; lecture honoraria from Vertex Pharmaceuticals; and travel support from Boehringer Ingelheim and Vertex Pharmaceuticals. The remaining authors declare that the research was conducted in the absence of any commercial or financial relationships that could be construed as a potential conflict of interest.

Acknowledgment

The authors greatly acknowledge funding from Mitacs Canada (IT19059) and Providence Healthcare (B. Tafech, S. Hedtrich) for the financial support. We also thank the Cystic Fibrosis Translational Research Centre at McGill for providing access to CF patient-derived cells harboring the 508del mutation. We further acknowledge financial support from the Deutsche Forschungsgemeinschaft (DFG, German Research Foundation) – Project ID 431232613 – SFB 1449 (S. Hedtrich, M. Mall), the Germany Federal Ministry of Education and Research (82DZL009C1 and 01GL2401A to M. Mall) and the Foundation Charité (S. Hedtrich). We would also like to thank Konrad Schmidt for the histological staining of 3D bronchial epithelial model and Gaëlle Wagner for her technical support of the HPRT assay and florescence microscopy. We also thank Dr. Bradley Quon (St. Paul's Hospital, Vancouver BC) for supporting the dornase alfa experiments.

Data availability

Data will be made available on request.

References

[1] R.C. Boucher, Muco-obstructive lung diseases, N. Engl. J. Med. 380 (20) (2019) 1941–1953, https://doi.org/10.1056/NEJMra1813799. From NLM.
[2] M.C. Bierlaagh, D. Muilwijk, J.M. Beekman, C.K. van der Ent, A new era for people with cystic fibrosis, Eur. J. Pediatr. 180 (9) (2021) 2731–2739, https://doi.org/10.1007/s00431-021-04168-y. From NLM.
[3] K.A. McBennett, P.B. Davis, M.W. Konstan, Increasing life expectancy in cystic fibrosis: advances and challenges, Pediatr. Pulmonol. 57 (Suppl. 1) (2022) S5–s12, https://doi.org/10.1002/ppul.25733. From NLM.
[4] M.A. Mall, P.R. Burgel, C. Castellani, J.C. Davies, M. Salathe, J.L. Taylor-Cousar, Cystic fibrosis, Nat. Rev. Dis. Primers 10 (1) (2024) 53, https://doi.org/10.1038/s41572-024-00538-6. From NLM.
[5] S. Cuevas Ocaña, N. El-Merhie, M.E. Kuipers, M. Lehmann, S.R. Enes, C. Voss, L.S. N. Dean, M. Loxham, A.W. Boots, S.M. Cloonan, et al., ERS International Congress 2022: highlights from the Basic and Translational Science Assembly, ERJ Open Res 9 (2) (2023), https://doi.org/10.1183/23120541.00561-2022. From NLM.
[6] K.B. Hisert, S.E. Birket, J.P. Clancy, D.G. Downey, J.F. Engelhardt, I. Fajac, R. D. Gray, M.E. Lachowicz-Scroggins, N. Mayer-Hamblett, P. Thibodeau, et al., Understanding and addressing the needs of people with cystic fibrosis in the era of CFTR modulator therapy, Lancet Respir. Med. 11 (10) (2023) 916–931, https://doi.org/10.1016/s2213-2600(23)00324-7 From NLM.
[7] S.Y. Graeber, C. Vitzthum, S.T. Pallenberg, L. Naehrlich, M. Stahl, A. Rohrbach, M. Drescher, R. Minso, F.C. Ringshausen, C. Rueckes-Nilges, et al., Effects of Elexacaftor/Tezacaftor/Ivacaftor therapy on CFTR function in patients with cystic fibrosis and one or two F508del alleles, Am. J. Respir. Crit. Care Med. 205 (5) (2022) 540–549, https://doi.org/10.1164/rccm.202110-2249OC. From NLM.
[8] L. Schaupp, A. Addante, M. Völler, K. Fentker, A. Kuppe, M. Bardua, J. Duerr, L. Piehler, J. Röhmel, S. Thee, et al., Longitudinal effects of elexacaftor/tezacaftor/ivacaftor on sputum viscoelastic properties, airway infection and inflammation in patients with cystic fibrosis, Eur. Respir. J. *62* (2) (2023), https://doi.org/10.1183/13993003.02153-2022. From NLM.
[9] M. Casey, C. Gabillard-Lefort, O.F. McElvaney, O.J. McElvaney, T. Carroll, R. C. Heeney, C. Gunaratnam, E.P. Reeves, M.P. Murphy, N.G. McElvaney, Effect of elexacaftor/tezacaftor/ivacaftor on airway and systemic inflammation in cystic fibrosis, Thorax 78 (8) (2023) 835–839, https://doi.org/10.1136/thorax-2022-219943. From NLM.
[10] M.H. Geurts, E. de Poel, G.D. Amatngalim, R. Oka, F.M. Meijers, E. Kruisselbrink, P. van Mourik, G. Berkers, K.M. de Winter-de Groot, S. Michel, et al., CRISPR-based adenine editors correct nonsense mutations in a cystic fibrosis organoid biobank, Cell Stem Cell 26 (4) (2020) 503–510 e507, https://doi.org/10.1016/j.stem.2020.01.019. From NLM Medline.
[11] G.A. Newby, D.R. Liu, In vivo somatic cell base editing and prime editing, Mol. Ther. 29 (11) (2021) 3107–3124, https://doi.org/10.1016/j.ymthe.2021.09.002. From NLM.
[12] B. Tafech, M.R. Rokhforouz, J. Leung, M.M. Sung, P.J. Lin, D.D. Sin, D. Lauster, S. Block, B.S. Quon, Y. Tam, et al., Exploring mechanisms of lipid nanoparticle-mucus interactions in healthy and cystic fibrosis conditions, Adv. Healthc. Mater. 13 (18) (2024) e2304525, https://doi.org/10.1002/adhm.202304525. From NLM.
[13] Y. Sun, S. Chatterjee, X. Lian, Z. Traylor, S.R. Sattiraju, Y. Xiao, S.A. Dilliard, Y. C. Sung, M. Kim, S.M. Lee, et al., In vivo editing of lung stem cells for durable gene correction in mice, Science 384 (6701) (2024) 1196–1202, https://doi.org/10.1126/science.adk9428. From NLM.
[14] M. Kesimer, A.A. Ford, A. Ceppe, G. Radicioni, R. Cao, C.W. Davis, C.M. Doerschuk, N.E. Alexis, W.H. Anderson, A.G. Henderson, et al., Airway mucin concentration as a marker of chronic bronchitis, N. Engl. J. Med. 377 (10) (2017) 911–922, https://doi.org/10.1056/NEJMoa1701632. From NLM.
[15] G.A. Duncan, J. Jung, A. Joseph, A.L. Thaxton, N.E. West, M.P. Boyle, J. Hanes, J. S. Suk, Microstructural alterations of sputum in cystic fibrosis lung disease, JCI Insight 1 (18) (2016) e88198, https://doi.org/10.1172/jci.insight.88198. From NLM.
[16] A.G. Henderson, C. Ehre, B. Button, L.H. Abdullah, L.H. Cai, M.W. Leigh, G. C. DeMaria, H. Matsui, S.H. Donaldson, C.W. Davis, et al., Cystic fibrosis airway secretions exhibit mucin hyperconcentration and increased osmotic pressure, J. Clin. Invest. 124 (7) (2014) 3047–3060, https://doi.org/10.1172/jci73469. From NLM.
[17] O. Lieleg, I. Vladescu, K. Ribbeck, Characterization of particle translocation through mucin hydrogels, Biophys. J. 98 (9) (2010) 1782–1789, https://doi.org/10.1016/j.bpj.2010.01.012. From NLM.

[18] R.S. Arzi, M. Davidovich-Pinhas, N. Cohen, A. Sosnik, An experimental and theoretical approach to understand the interaction between particles and mucosal tissues, Acta Biomater. 158 (2023) 449–462, https://doi.org/10.1016/j.actbio.2022.12.060. From NLM.

[19] J. Hansing, C. Ciemer, W.K. Kim, X. Zhang, J.E. DeRouchey, R.R. Netz, Nanoparticle filtering in charged hydrogels: effects of particle size, charge asymmetry and salt concentration, Eur. Phys. J. E Soft Matter 39 (5) (2016) 53, https://doi.org/10.1140/epje/i2016-16053-2. From NLM.

[20] D.B. Hill, R.F. Long, W.J. Kissner, E. Atieh, I.C. Garbarine, M.R. Markovetz, N. C. Fontana, M. Christy, M. Habibpour, R. Tarran, et al., Pathological mucus and impaired mucus clearance in cystic fibrosis patients result from increased concentration, not altered pH, Eur. Respir. J. 6 (2018) 52, https://doi.org/10.1183/13993003.01297-2018. From NLM.

[21] D.B. Hill, B. Button, M. Rubinstein, R.C. Boucher, Physiology and pathophysiology of human airway mucus, Physiol. Rev. 102 (4) (2022) 1757–1836, https://doi.org/10.1152/physrev.00004.2021. From NLM.

[22] A. Akinc, M.A. Maier, M. Manoharan, K. Fitzgerald, M. Jayaraman, S. Barros, S. Ansell, X. Du, M.J. Hope, T.D. Madden, et al., The Onpattro story and the clinical translation of nanomedicines containing nucleic acid-based drugs, Nat. Nanotechnol. 14 (12) (2019) 1084–1087, https://doi.org/10.1038/s41565-019-0591-y.

[23] P.R. Cullis, P.L. Felgner, The 60-year evolution of lipid nanoparticles for nucleic acid delivery, Nat. Rev. Drug Discov. 23 (9) (2024) 709–722, https://doi.org/10.1038/s41573-024-00977-6. From NLM.

[24] P.P. Adhikary, Q. Ul Ain, A.C. Hocke, S. Hedtrich, COVID-19 highlights the model dilemma in biomedical research, Nat. Rev. Mater. (2021) 1–3, https://doi.org/10.1038/s41578-021-00305-z. From NLM.

[25] D. Fakih, A.M. Rodriguez-Piñeiro, S. Trillo-Muyo, C.M. Evans, A. Ermund, G. C. Hansson, Normal murine respiratory tract has its mucus concentrated in clouds based on the Muc5b mucin, Am. J. Phys. Lung Cell. Mol. Phys. 318 (6) (2020) L1270–l1279, https://doi.org/10.1152/ajplung.00485.2019. From NLM.

[26] C.S. Rogers, W.M. Abraham, K.A. Brogden, J.F. Engelhardt, J.T. Fisher, P.B. Jr. McCray, G. McLennan, D.K. Meyerholz, E. Namati, L.S. Ostedgaard, et al., The porcine lung as a potential model for cystic fibrosis, Am. J. Phys. Lung Cell. Mol. Phys. 295 (2) (2008) L240–L263, https://doi.org/10.1152/ajplung.90203.2008. From NLM.

[27] J. Bolsoni, D. Liu, F. Mohabatpour, R. Ebner, G. Sadhnani, B. Tafech, J. Leung, S. Shanta, K. An, T. Morin, et al., Lipid nanoparticle-mediated hit-and-run approaches yield efficient and safe in situ gene editing in human skin, ACS Nano 17 (21) (2023) 22046–22059, https://doi.org/10.1021/acsnano.3c08644. From NLM.

[28] D.P. Dever, R.O. Bak, A. Reinisch, J. Camarena, G. Washington, C.E. Nicolas, M. Pavel-Dinu, N. Saxena, A.B. Wilkens, S. Mantri, et al., CRISPR/Cas9 β-globin gene targeting in human haematopoietic stem cells, Nature 539 (7629) (2016) 384–389, https://doi.org/10.1038/nature20134. From NLM.

[29] A. Lattanzi, V. Meneghini, G. Pavani, F. Amor, S. Ramadier, T. Felix, C. Antoniani, C. Masson, O. Alibeu, C. Lee, et al., Optimization of CRISPR/Cas9 delivery to human hematopoietic stem and progenitor cells for therapeutic genomic rearrangements, Mol. Ther. 27 (1) (2019) 137–150, https://doi.org/10.1016/j.ymthe.2018.10.008. From NLM.

[30] J.L. Everman, C. Rios, M.A. Seibold, Primary airway epithelial cell gene editing using CRISPR-Cas9, Methods Mol. Biol. 1706 (2018) 267–292, https://doi.org/10.1007/978-1-4939-7471-9_15. From NLM.

[31] K.D. Koh, S. Siddiqui, D. Cheng, L.R. Bonser, D.I. Sun, L.T. Zlock, W.E. Finkbeiner, P.G. Woodruff, D.J. Erle, Efficient RNP-directed human gene targeting reveals SPDEF is required for IL-13-induced Mucostasis, Am. J. Respir. Cell Mol. Biol. 62 (3) (2020) 373–381, https://doi.org/10.1165/rcmb.2019-0266OC. From NLM.

[32] S. Krishnamurthy, C. Wohlford-Lenane, S. Kandimalla, G. Sartre, D.K. Meyerholz, V. Théberge, S. Hallée, A.M. Duperré, T. Del'Guidice, J.P. Lepetit-Stoffaes, et al., Engineered amphiphilic peptides enable delivery of proteins and CRISPR-associated nucleases to airway epithelia, Nat. Commun. 10 (1) (2019) 4906, https://doi.org/10.1038/s41467-019-12922-y. From NLM.

[33] R. Rapiteanu, T. Karagyozova, N. Zimmermann, K. Singh, G. Wayne, M. Martufi, N. N. Belyaev, E.M. Hessel, D. Michalovich, R. Macarron, et al., Highly efficient genome editing in primary human bronchial epithelial cells differentiated at air-liquid interface, Eur. Respir. J. 5 (2020) 55, https://doi.org/10.1183/13993003.00950-2019. From NLM.

[34] S. Suzuki, A.M. Crane, V. Anirudhan, C. Barillà, N. Matthias, S.H. Randell, A. Rab, E.J. Sorscher, J.L. Kerschner, S. Yin, et al., Highly efficient gene editing of cystic fibrosis patient-derived airway basal cells results in functional CFTR correction, Mol. Ther. 28 (7) (2020) 1684–1695, https://doi.org/10.1016/j.ymthe.2020.04.021. From NLM.

[35] S. Vaidyanathan, A.A. Salahudeen, Z.M. Sellers, D.T. Bravo, S.S. Choi, A. Batish, W. Le, R. Baik, de la S. O., M.P. Kaushik, et al., High-Efficiency, Selection-free Gene Repair in Airway Stem Cells from Cystic Fibrosis Patients Rescues CFTR Function in Differentiated Epithelia, Cell Stem Cell 26 (2) (2020), https://doi.org/10.1016/j.stem.2019.11.002, 161–171.e164. From NLM.

[36] U. Griesenbach, E.W. Alton, Gene transfer to the lung: lessons learned from more than 2 decades of CF gene therapy, Adv. Drug Deliv. Rev. 61 (2) (2009) 128–139, https://doi.org/10.1016/j.addr.2008.09.010. From NLM.

[37] R.C. Fleith, H.V. Mears, X.Y. Leong, T.J. Sanford, E. Emmott, S.C. Graham, D. S. Mansur, T.R. Sweeney, IFIT3 and IFIT2/3 promote IFIT1-mediated translation inhibition by enhancing binding to non-self RNA, Nucleic Acids Res. 46 (10) (2018) 5269–5285, https://doi.org/10.1093/nar/gky191. From NLM.

[38] M. Habjan, P. Hubel, L. Lacerda, C. Benda, C. Holze, C.H. Eberl, A. Mann, E. Kindler, C. Gil-Cruz, J. Ziebuhr, et al., Sequestration by IFIT1 impairs translation of 2'O-unmethylated capped RNA, PLoS Pathog. 9 (10) (2013) e1003663, https://doi.org/10.1371/journal.ppat.1003663. From NLM.

[39] J. Gilleron, W. Querbes, A. Zeigerer, A. Borodovsky, G. Marsico, U. Schubert, K. Manygoats, S. Seifert, C. Andree, M. Stöter, et al., Image-based analysis of lipid nanoparticle-mediated siRNA delivery, intracellular trafficking and endosomal escape, Nat. Biotechnol. 31 (7) (2013) 638–646, https://doi.org/10.1038/nbt.2612. From NLM.

[40] M. Maugeri, M. Nawaz, A. Papadimitriou, A. Angerfors, A. Camponeschi, M. Na, M. Hölttä, P. Skantze, S. Johansson, M. Sundqvist, et al., Linkage between endosomal escape of LNP-mRNA and loading into EVs for transport to other cells, Nat. Commun. 10 (1) (2019) 4333, https://doi.org/10.1038/s41467-019-12275-6. From NLM.

[41] M. Schlich, R. Palomba, G. Costabile, S. Mizrahy, M. Pannuzzo, D. Peer, P. Decuzzi, Cytosolic delivery of nucleic acids: the case of ionizable lipid nanoparticles, Bioeng Transl Med 6 (2) (2021) e10213, https://doi.org/10.1002/btm2.10213. From NLM.

[42] L. Zheng, S.R. Bandara, Z. Tan, C. Leal, Lipid nanoparticle topology regulates endosomal escape and delivery of RNA to the cytoplasm, Proc. Natl. Acad. Sci. USA 120 (27) (2023) e2301067120, https://doi.org/10.1073/pnas.2301067120. From NLM.

[43] J.A. Müller, N. Schäffler, T. Kellerer, G. Schwake, T.S. Ligon, J.O. Rädler, Kinetics of RNA-LNP delivery and protein expression, Eur. J. Pharm. Biopharm. 197 (2024) 114222, https://doi.org/10.1016/j.ejpb.2024.114222. From NLM.

[44] M. Herrera, J. Kim, Y. Eygeris, A. Jozic, G. Sahay, Illuminating endosomal escape of polymorphic lipid nanoparticles that boost mRNA delivery, Biomater. Sci. 9 (12) (2021) 4289–4300, https://doi.org/10.1039/d0bm01947j. From NLM.

[45] P. Paramasivam, C. Franke, M. Stöter, A. Höijer, S. Bartesaghi, A. Sabirsh, L. Lindfors, M.Y. Arteta, A. Dahlén, A. Bak, et al., Endosomal escape of delivered mRNA from endosomal recycling tubules visualized at the nanoscale, J. Cell Biol. 2 (2022) 221, https://doi.org/10.1083/jcb.202110137. From NLM.

[46] K. Karikó, M. Buckstein, H. Ni, D. Weissman, Suppression of RNA recognition by toll-like receptors: the impact of nucleoside modification and the evolutionary origin of RNA, Immunity 23 (2) (2005) 165–175, https://doi.org/10.1016/j.immuni.2005.06.008. From NLM.

[47] J.D. Finn, A.R. Smith, M.C. Patel, L. Shaw, M.R. Youniss, J. van Heteren, T. Dirstine, C. Ciullo, R. Lescarbeau, J. Seitzer, et al., A single administration of CRISPR/Cas9 lipid nanoparticles achieves robust and persistent in vivo genome editing, Cell Rep. 22 (9) (2018) 2227–2235, https://doi.org/10.1016/j.celrep.2018.02.014. From NLM.

[48] H. Panjideh, N. Niesler, A. Weng, H. Fuchs, Improved Therapy of B-Cell Non-Hodgkin Lymphoma by Obinutuzumab-Dianthin Conjugates in Combination with the Endosomal Escape Enhancer SO1861, Toxins (Basel) *14* (7) (2022), https://doi.org/10.3390/toxins14070478. From NLM.

[49] S. Chatterjee, E. Kon, P. Sharma, D. Peer, Endosomal escape: a bottleneck for LNP-mediated therapeutics, Proc. Natl. Acad. Sci. USA 121 (11) (2024) e2307800120, https://doi.org/10.1073/pnas.2307800120. From NLM.

[50] R. Charbaji, M. Kar, L.E. Theune, J. Bergueiro, M. Calderon, S. Hedtrich, Design and testing of efficient mucus-penetrating nanogels - pitfalls of preclinical testing and lessons learned, Small (2021), https://doi.org/10.1002/smll.202007963.

[51] S. Silva, J. Bicker, A. Falcão, A. Fortuna, Air-liquid interface (ALI) impact on different respiratory cell cultures, Eur. J. Pharm. Biopharm. 184 (2023) 62–82, https://doi.org/10.1016/j.ejpb.2023.01.013.

[52] C. Clary-Meinesz, J. Mouroux, P. Huitorel, J. Cosson, D. Schoevaert, B. Blaive, Ciliary beat frequency in human bronchi and bronchioles, CHEST 111 (3) (1997) 692–697, https://doi.org/10.1378/chest.111.3.692 (acccessed 2025/06/05).

[53] J. Yager, T.-M. Chen, M.J. Dulfano, Measurement of frequency of ciliary beats of human respiratory epithelium, Chest 73 (5) (1978) 627–633, https://doi.org/10.1378/chest.73.5.627 (acccessed 2025/06/05).

[54] J. Parker, S. Sarlang, S. Thavagnanam, G. Williamson, D. O'Donoghue, R. Villenave, U. Power, M. Shields, L. Heaney, G. Skibinski, A 3-D well-differentiated model of pediatric bronchial epithelium demonstrates unstimulated morphological differences between asthmatic and nonasthmatic cells, Pediatr. Res. 67 (1) (2010) 17–22, https://doi.org/10.1203/PDR.0b013e3181c0b200.

[55] L. Wei, J. Zhao, J. Bao, Y. Ma, Y. Shang, Z. Gao, The characteristics and clinical significance of mucin levels in bronchoalveolar lavage fluid of patients with interstitial lung disease, J. Investig. Med. 67 (4) (2019) 761–766, https://doi.org/10.1136/jim-2018-000785. From NLM.

[56] H.K. Okur, K. Yalcin, C. Tastan, S. Demir, B. Yurtsever, G.S. Karakus, D.D. Kancagi, S. Abanuz, U. Seyis, R. Zengin, et al., Preliminary report of in vitro and in vivo effectiveness of dornase alfa on SARS-CoV-2 infection, New Microbes New Infect 37 (2020) 100756, https://doi.org/10.1016/j.nmni.2020.100756. From NLM.

[57] M. Bulcaen, P. Kortleven, R.B. Liu, G. Maule, E. Dreano, M. Kelly, M.M. Ensinck, S. Thierie, M. Smits, M. Ciciani, et al., Prime editing functionally corrects cystic fibrosis-causing CFTR mutations in human organoids and airway epithelial cells, Cell Rep Med 5 (5) (2024) 101544, https://doi.org/10.1016/j.xcrm.2024.101544. From NLM.

[58] S.L. Farmen, P.H. Karp, P. Ng, D.J. Palmer, D.R. Koehler, J. Hu, A.L. Beaudet, J. Zabner, M.J. Welsh, Gene transfer of CFTR to airway epithelia: low levels of expression are sufficient to correct cl- transport and overexpression can generate basolateral CFTR, Am. J. Phys. Lung Cell. Mol. Phys. 289 (6) (2005) L1123–L1130, https://doi.org/10.1152/ajplung.00049.2005. From NLM.

[59] T. Wei, Y. Sun, Q. Cheng, S. Chatterjee, Z. Traylor, L.T. Johnson, M.L. Coquelin, J. Wang, M.J. Torres, X. Lian, et al., Lung SORT LNPs enable precise homology-directed repair mediated CRISPR/Cas genome correction in cystic fibrosis models, Nat. Commun. 14 (1) (2023) 7322, https://doi.org/10.1038/s41467-023-42948-2. From NLM.

[60] D. Roth, A.T. Şahin, F. Ling, N. Tepho, C.N. Senger, E.J. Quiroz, B.A. Calvert, A. M. van der Does, T.G. Güney, S. Glasl, et al., Structure and function relationships of mucociliary clearance in human and rat airways, Nat. Commun. 16 (1) (2025) 2446, https://doi.org/10.1038/s41467-025-57667-z. From NLM.
[61] S.M. Rowe, J.B. Zuckerman, D. Dorgan, J. Lascano, K. McCoy, M. Jain, M. S. Schechter, S. Lommatzsch, V. Indihar, N. Lechtzin, et al., Inhaled mRNA therapy for treatment of cystic fibrosis: interim results of a randomized, double-blind, placebo-controlled phase 1/2 clinical study, J. Cyst. Fibros. 22 (4) (2023) 656–664, https://doi.org/10.1016/j.jcf.2023.04.008. From NLM.
[62] N.M. Gaudelli, A.C. Komor, H.A. Rees, M.S. Packer, A.H. Badran, D.I. Bryson, D. R. Liu, Programmable base editing of a*T to G*C in genomic DNA without DNA cleavage, Nature 551 (7681) (2017) 464–471, https://doi.org/10.1038/nature24644.
[63] S. Jin, Y. Zong, Q. Gao, Z. Zhu, Y. Wang, P. Qin, C. Liang, D. Wang, J.L. Qiu, F. Zhang, et al., Cytosine, but not adenine, base editors induce genome-wide off-target mutations in rice, Science 364 (6437) (2019) 292–295, https://doi.org/10.1126/science.aaw7166.
[64] E. Zuo, Y. Sun, W. Wei, T. Yuan, W. Ying, H. Sun, L. Yuan, L.M. Steinmetz, Y. Li, H. Yang, Cytosine base editor generates substantial off-target single-nucleotide variants in mouse embryos, Science 364 (6437) (2019) 289–292, https://doi.org/10.1126/science.aav9973.
[65] R.T. Walton, K.A. Christie, M.N. Whittaker, B.P. Kleinstiver, Unconstrained genome targeting with near-PAMless engineered CRISPR-Cas9 variants, Science 368 (6488) (2020) 290–296, https://doi.org/10.1126/science.aba8853. From NLM.
[66] M.F. Richter, K.T. Zhao, E. Eton, A. Lapinaite, G.A. Newby, B.W. Thuronyi, C. Wilson, L.W. Koblan, J. Zeng, D.E. Bauer, et al., Phage-assisted evolution of an adenine base editor with improved Cas domain compatibility and activity, Nat. Biotechnol. 38 (7) (2020) 883–891, https://doi.org/10.1038/s41587-020-0453-z. From NLM Medline.
[67] D. Yan, B. Ren, L. Liu, F. Yan, S. Li, G. Wang, W. Sun, X. Zhou, H. Zhou, High-efficiency and multiplex adenine base editing in plants using new TadA variants, Mol. Plant 14 (5) (2021) 722–731, https://doi.org/10.1016/j.molp.2021.02.007. From NLM.
[68] A. Fritsch, S. Loeckermann, J.S. Kern, A. Braun, M.R. Bösl, T.A. Bley, H. Schumann, D. von Elverfeldt, D. Paul, M. Erlacher, et al., A hypomorphic mouse model of dystrophic epidermolysis bullosa reveals mechanisms of disease and response to fibroblast therapy, J. Clin. Invest. 118 (5) (2008) 1669–1679, https://doi.org/10.1172/jci34292. From NLM.
[69] A. Addante, W. Raymond, I. Gitlin, A. Charbit, X. Orain, A.W. Scheffler, A. Kuppe, J. Duerr, M. Daniltchenko, M. Drescher, et al., A novel thiol-saccharide mucolytic for the treatment of muco-obstructive lung diseases, Eur. Respir. J. 5 (2023) 61, https://doi.org/10.1183/13993003.02022-2022. From NLM.
[70] J. Arenhoevel, A. Kuppe, A. Addante, L.F. Wei, N. Boback, C. Butnarasu, Y. Zhong, C. Wong, S.Y. Graeber, J. Duerr, et al., Thiolated polyglycerol sulfate as potential mucolytic for muco-obstructive lung diseases, Biomater. Sci. 12 (17) (2024) 4376–4385, https://doi.org/10.1039/d4bm00381k. From NLM.
[71] C.M. Zimmermann, L. Deßloch, D.C. Jürgens, P. Luciani, O.M. Merkel, Evaluation of the effects of storage conditions on spray-dried siRNA-LNPs before and after subsequent drying, Eur. J. Pharm. Biopharm. 193 (2023) 218–226, https://doi.org/10.1016/j.ejpb.2023.11.007.
[72] H. Miao, K. Huang, Y. Li, R. Li, X. Zhou, J. Shi, Z. Tong, Z. Sun, A. Yu, Optimization of formulation and atomization of lipid nanoparticles for the inhalation of mRNA, Int. J. Pharm. 640 (2023) 123050, https://doi.org/10.1016/j.ijpharm.2023.123050. From NLM.
[73] H.-Y. Li, A. Paramanandana, S.Y. Kim, L. Granger, B.T. Raimi-Abraham, R. Shattock, C. Makatsoris, B. Forbes, Targeted nasal delivery of LNP-mRNAs aerosolised by Rayleigh breakup technology, Int. J. Pharm. 672 (2025) 125335, https://doi.org/10.1016/j.ijpharm.2025.125335.
[74] J.A. Kulkarni, S.B. Thomson, J. Zaifman, J. Leung, P.K. Wagner, A. Hill, Y.Y. C. Tam, P.R. Cullis, T.L. Petkau, B.R. Leavitt, Spontaneous, solvent-free entrapment of siRNA within lipid nanoparticles, Nanoscale 12 (47) (2020) 23959–23966, https://doi.org/10.1039/d0nr06816k. From NLM.
[75] R. Gilabert-Oriol, M. Thakur, K. Haussmann, N. Niesler, C. Bhargava, C. Görick, H. Fuchs, A. Weng, Saponins from Saponaria officinalis L. augment the efficacy of a rituximab-immunotoxin, Planta Med. 82 (18) (2016) 1525–1531, https://doi.org/10.1055/s-0042-110495. From NLM.
[76] A. Dobin, C.A. Davis, F. Schlesinger, J. Drenkow, C. Zaleski, S. Jha, P. Batut, M. Chaisson, T.R. Gingeras, STAR: ultrafast universal RNA-seq aligner, Bioinformatics 29 (1) (2013) 15–21, https://doi.org/10.1093/bioinformatics/bts635. From NLM.
[77] Y. Liao, G.K. Smyth, W. Shi, featureCounts: an efficient general purpose program for assigning sequence reads to genomic features, Bioinformatics 30 (7) (2013) 923–930, https://doi.org/10.1093/bioinformatics/btt656 (accessed 7/11/2023).
[78] J. Zyla, M. Marczyk, T. Domaszewska, S.H.E. Kaufmann, J. Polanska, J. Weiner, Gene set enrichment for reproducible science: comparison of CERNO and eight other algorithms, Bioinformatics 35 (24) (2019) 5146–5154, https://doi.org/10.1093/bioinformatics/btz447. From NLM.
[79] S.Y. Graeber, A. Balázs, N. Ziegahn, T. Rubil, C. Vitzthum, L. Piehler, M. Drescher, K. Seidel, A. Rohrbach, J. Röhmel, et al., Personalized CFTR modulator therapy for G85E and N1303K homozygous patients with cystic fibrosis, Int. J. Mol. Sci. 15 (2023) 24, https://doi.org/10.3390/ijms241512365. From NLM.